A transition in atmospheric emissions of particles and gases from on-road heavy-duty trucks

Liyuan Zhou[1], Åsa M. Hallquist[2*], Mattias Hallquist[3], Christian M. Salvador[3], Samuel M. Gaita[3], Åke Sjödin[2], Martin Jerksjö[2], Håkan Salberg[2], Ingvar Wängberg[2], Johan Mellqvist[4], Qianyun Liu[1], Berto P. Lee[1], Chak K. Chan[1*]

[1]School of Energy and Environment, City University of Hong Kong, Hong Kong, China
[2]IVL Swedish Environmental Research Institute, Gothenburg, Sweden
[3]Department of Chemistry and Molecular Biology, University of Gothenburg, Gothenburg, Sweden
[4] Earth and Space Sciences, Chalmers University of Technology, Gothenburg, Sweden

Correspondence to: Åsa M. Hallquist (asa.hallquist@ivl.se), Chak K. Chan (Chak.K.Chan@cityu.edu.hk)

Abstract. The transition in extent and characteristics of atmospheric emissions caused by the modernisation of the heavy-duty on-road fleet were studied utilising roadside measurements. Emissions of particle number (PN), particle mass (PM), black carbon (BC), nitrogen oxides (NO_x), carbon monoxide (CO), hydrocarbon (HC), particle size distributions and particle volatility were measured from 556 individual heavy-duty trucks (HDTs). Substantial reductions in PM, BC, NO_x, CO and to a lesser extent PN were observed from Euro III to Euro VI HDTs by 99%, 98%, 93% and 57% for the average emissions factors of PM, BC, NO_x, and CO respectively. Despite significant total reductions in NO_x emissions, the fraction of NO_2 in the NO_x emissions increased continuously from Euro IV to Euro VI HDTs. Larger data scattering was evident for PN emissions in comparison to solid particle number (SPN) for Euro VI HDTs, indicating a highly variable fraction of volatile particle components. Particle size distributions of Euro III to EEV HDTs were bimodal, whereas those of Euro VI HDTs were nucleation mode dominated. High emitters disproportionately contributed to a large fraction of the total emissions with the highest-emitting 10% of HDTs in each pollutant category being responsible for 65% of total PM, 70% of total PN and 44% of total NO_x emissions, respectively. Euro VI HDTs, which accounted for 53% of total kilometres driven by Swedish HDTs, were estimated to only contribute to 2%, 6%, 12% and 47% of PM, BC, NO_x, and PN emissions. A shift to a Euro VI HDTs dominant fleet would promote a transition of atmospheric emissions towards low PM, BC, NO_x, and CO levels. Nonetheless, reducing PN, SPN, and NO_2 emissions from Euro VI HDTs is still important to improve air quality in urban environments.

1 Introduction

Vehicular emissions contribute significantly to gaseous and particle pollutants in the urban atmosphere and description of their extent and characteristics are key input components for urban air quality modelling. As technology and traffic demands change, so do the characteristics of the emissions. In Europe, the introduction of new legislation, especially Euro VI, has aimed to reduce emissions of many pollutants. Legislation exists for particles (mass and number) and selected gases, however, there are also many components of the emissions that are not directly regulated but are potentially detrimental to human health. The most notable example of a non-regulated pollutant is the abundance of ultrafine particles (UFP) (Campagnolo et al., 2019), defined as particles with a diameter less than 100 nm (Zhu et al., 2002). UFPs can cause lung disease, an increase of blood coagulability and cardiovascular disease and related mortality (Du et al., 2016). In the most recent Euro class, this has partly been covered by introducing a limit on the solid particle number (SPN) while volatile particles and particles less than 23 nm are not considered. Furthermore, the legislation has mainly been based on test cycles performed before introducing a new engine into the market but only recently also off-cycle and in-service conformity testing has been introduced, hence the actual performance in real-traffic is less constrained, where driving pattern, maintenance, and age of engine will vary. Here real-traffic studies may capture variability between vehicles and also put the effect of new legislation and parallel phase-out of older technology into perspective for the abatement of urban air pollution.

Heavy-duty vehicles (HDVs) usually account for a smaller number fraction of on-road vehicles than light-duty vehicles but they tend to contribute to a disproportionately high fraction of mobile source particulate matter emissions (Gertler, 2005; Cui et al., 2017). Emissions from HDVs, often diesel, are significantly affected by the engine type, exhaust after-treatment system (ATS), and driving conditions. The main purpose of ATS is the reduction of particulate and gaseous pollutants. Diesel Oxidation Catalysts (DOC) are used for reducing hydrocarbon emissions, selective catalytic reduction (SCR) systems or exhaust gas recirculation (EGR) are employed to mitigate NO_x emissions, and diesel particulate filters (DPF) can reduce particulate matter mass emissions. The use of ATS can, however, bring undesired side effects. For example, conversion of SO_2 to SO_3 and increased gaseous sulfuric acid formation have been reported from DOCs (Arnold et al., 2012). DPFs potentially enhance the formation of UFP (Herner et al., 2011; Preble et al., 2017). Retrofitted DPF can slightly reduce the NO_x emissions but significantly increase the direct emission of NO_2 by as much as a factor of 8 (Smith et al., 2019). Failure of the temperature-dependent SCR in eliminating the excess NO_2 leads to an elevated NO_2 to NO_x ratio (Herner et al., 2009; Bishop et al., 2010; He et al., 2015).

The Euro standard regulates vehicle emission limits in Europe. The Euro III standard was established in 1999, and more stringent Euro IV and Euro V standards were implemented in 2005 and 2008, respectively. The Enhanced Environmentally Friendly Vehicle (EEV) is a voluntary environmental standard which lies between the levels of Euro V and Euro VI. The currently enforced Euro VI standard has been implemented since 2013-2014 and introduced SPN limits into the regulation for the first time. Generally, newer engines are expected to perform better in controlling pollutant emissions. Guo et al. (2014) reported that Euro V diesel buses performed better than Euro IV and Euro III diesel buses in the emissions of all the pollutants, except for the generation of more nucleation mode particles. The latest 2018 European Environmental Agency (EEA) report confirms an overall improvement in the European air quality, while the road transport sector remains one of the major contributors to pollutant emissions and the largest contributor to the total NO_x emission (Grigoratos et al., 2019; EEA, 2018). A recent on-board sensor-based study pointed out that HDVs emitted more than three times the NO_x certification standard during real-world hot-driving and idling operations (Tan et al., 2019). Published data regarding particle and gaseous pollutant emissions from real-world on-road Euro VI heavy-duty vehicles are scarce and often limited by the small sample size (Giechaskiel et al., 2018; Grigoratos et al., 2019; Moody and Tate, 2017). Remote sensing sampling can measure a large sample size of vehicles but are usually restricted to gaseous pollutant emissions (Burgard and Provinsal, 2009; Burgard et al., 2006; Carslaw et al., 2011). From an air quality perspective, the particle emissions are crucial. The complexity and dynamics of atmospheric particles require detailed information of its emission for atmospheric modelling and for descriptions of their health impacts. For example, particle size is important to determine the effects on respiratory deposition in humans (Manigrasso et al., 2017; Lv et al., 2016).

Diesel exhaust particles are a complex mixture of numerous semi-volatile and non-volatile species, and the semi-volatile compounds will experience gas-to-particle partitioning in the atmosphere (Robinson et al., 2007; Donahue et al., 2006). Biswas et al. (2009) reported that the semi-volatile fraction in HDV emission is more oxidative than the refractory particles, which may change the redox state in cells and cause oxidative stress. Semi-volatile organic compounds, such as PAHs and their derivatives may possess genotoxic and carcinogenic characteristics (Bocchi et al., 2016; Vojtisek-Lom et al., 2015). Giechaskiel et al. (2009) suggested using the volatile mass fraction as a metric to assess health effects as the volatile mass dissolves in the lung fluid and thereby interacts with epithelial cells. Deploying a Volatility Tandem Differential Mobility Analyzer in suburban Guangzhou, China, Cheung et al. (2016) found that 57–71 % of ambient particles between 40 and 300 nm contain volatile components. Furthermore, the evaporated semi-volatile compounds from the particle phase can be further oxidized to form secondary organic aerosols (SOA) (Hallquist et al., 2009; Gentner et al., 2017). To better quantify the health effects and global and regional contributions of road traffic to the total particle burden in the atmosphere, information on the volatility properties of vehicle particulate emissions is needed.

Different approaches have been applied to study the emissions from HDTs (Franco et al., 2013). Chassis dynamometer tests provide relatively comprehensive emission characteristics of individual vehicles (Jiang et al., 2018; Chen et al., 2018; Thiruvengadam et al., 2015), but the artificial driving cycles make it difficult to simulate the full range of real-world driving conditions. Portable emission measurement systems (PEMS) (Grigoratos et al., 2019; Pirjola et al., 2017) and plume chasing studies (Lau et al., 2015; Pirjola et al., 2016) have been conducted in real-world environments but are often limited by small sample sizes. Tunnel studies (Li et al., 2018) measure the average emission of all vehicles passing through the tunnel without specific emission information of vehicle types. Roadside measurements, as presented in this study, provide an opportunity to study real-world on-road traffic emissions on large sample sizes with individual vehicle information (e.g. Hallquist et al., 2013; Dallmann et al., 2012; Carslaw and Rhys-Tyler, 2013; Watne et al., 2018).

In this work, we measured the gaseous and particle emissions from 556 on-road individual HDTs and quantified changes in emissions and the potential transition in characteristics caused by the reduction achieved by the introduction of more stringent Euro standards. Particle size distributions and particle volatilities were investigated with respect to Euro class, and pollutant emission characteristics were studied with respect to year of registration. Cumulative pollutant distributions were established to demonstrate the importance of controlling high-emitters in reducing total emissions. The typical contribution of air pollution emissions from each Euro class HDTs was estimated based on total vehicle kilometres driven. Results of the presented pollutant emission factors in our study will be useful for both emission models and emission inventories. A clear transition of atmospheric pollutant emission trends was evident and can provide useful guidance for policies regarding the regulation of existing fleets.

2 Methods

2.1 Field sampling site

Pollutant emissions from HDTs were measured at a roadside location in Gothenburg, Sweden (Fig. 1). The HDTs passed the sampling location with an average speed of 27 km h^{-1} and acceleration of 0.7 km h^{-1} s^{-1} on a slight uphill slope (~2°). Under such uphill driving conditions, vehicles are expected to emit higher levels of pollutants than during downhill and cruise driving. This will be further examined in Sect. 3.3.

2.2 Air sampling

The sampling of the emissions was conducted in line with Hallquist et al. (2013), i.e. extractive sampling of passing HDT plumes. Air was continuously drawn through a flexible copper tube to the instruments inside a container. A similar experimental set-up was previously applied to on-road bus emission measurements (Liu et al., 2019). Particles were measured by an EEPS (Engine Exhaust Particle Sizer, Model 3090 TSI Inc.) in the size range of 5.6-560 nm with high time resolution (10 Hz) while total particle number was measured by a butanol-based condensation particle counter (CPC Model 3775 TSI Inc., 50 cut-off diameter 4 nm). Particle numbers measured by the two instruments showed a good correlation (R^2=0.73) (Fig. S1). A second EEPS measured the outflow of a TD (thermodenuder, Dekati, Inc.), enabling estimations of particle volatility. The data were corrected for size-dependent losses in the TD. The temperature inside the TD heating zone was set to 250°C with a residence time of ~ 0.6 s, which is generally sufficient to evaporate nearly all the organics and sulphates from the particles (Huffman et al., 2008). However, organics with extremely low volatility (organic saturation mass concentration, $C^* < 10^{-5}$µg m^{-3} at 298 K) may still be retained even at this high temperature (Gkatzelis et al., 2016). Thus, in this study, we define the 'non-volatile components' as particle components that remain after passing through the TD operating at 250°C. Differences in counting efficiencies between the two EEPS were accounted for by size-dependent correction factors (typically less than 10%), which were retrieved by simultaneous sampling of ammonium sulphate particles by both EEPS and direct comparison of their measured size distributions (Fig. S2). BC and the mixture of BC and brown carbon (BrC) were measured by an Aethalometer at 880 nm and 370 nm respectively (Model AE 33, Magee Scientific Inc.). The determination of particle mass concentrations by the integrated particle size distribution (IPSD) method requires information on particle density. Particle sphericity and unit density were assumed due to a lack of detailed knowledge about the chemical composition of the emitted particles. Figure S3 shows that there is a good linear relationship at EF_{PM} larger than 1 mg (kg fuel)$^{-1}$ between the BC mass measured by the Aethalometer and the non-volatile particle mass measured by the EEPS but assuming sphericity and unit density the EEPS mass is lower, which indicates a potential underestimation of the effective non-volatile particle density. Compared to the EEPS, the detection limit of the Aethalometer is five times higher, which may influence the correlation between BC and PM at low mass loading conditions (Fig. S3). There have been several studies on the morphology and density of combustion generated particles and its detailed dependence on combustion and dilution condition (e.g. Maricq and Ning, 2004; Ristimaki et al., 2007; Liu et al., 2009; Zheng et al., 2011; Quiros et al., 2015). However, to be consistent, avoid assumptions and to compare with a majority of previously reported data, unity density was used for further discussion and comparisons. CO_2 was measured by a non-dispersive infrared gas analyser (LI-840, LI-COR Inc.). NO_x and NO were measured simultaneously by two separate chemiluminescent analysers (Model 42i, Thermo Scientific Inc.), and the NO_2 concentration was calculated from the difference between the NO_x and NO concentrations. SO_2 was measured by a pulsed fluorescence gas analyser (Model 43c, Thermo Scientific Inc.). A Remote Sensing Device (RSD) (OPUS Inspection Inc.) was used to measure the gaseous emission factors of CO, NO_x, and HC. Briefly, the instrument was set up with a transmitter and a receiver on the same side of the truck passing lane and a reflector on the opposite side. Co-linear beams of IR and UV light are emitted and cross-reflected through the plume and light attenuation related to respective pollutant concentrations are measured. Gas pollutant concentrations were determined relative to CO_2 as measured by the RSD. NO_x and NO measured by the gas analysers and the RSD were in agreement (R^2=0.53 and 0.66 respectively, Figs. S4, S8a). The High-Resolution Time-of-Flight Chemical Ionization Mass Spectrometer (HR-ToF-CIMS) shown in Fig. 1 was used to characterise the chemical composition of organic and inorganic compounds in the gas and particle phase, emitted from the HDTs. However, the extensive chemical characterisation is beyond the scope of this work and will be presented elsewhere.

A schematic of the experimental setup is given in Fig. 1 along with some examples of typical temporal profiles of pollutant concentrations in the plumes from Euro III and Euro VI HDTs. A camera at the roadside recorded the HDT plate numbers, which was used for identification and to obtain engine Euro type information. All the instruments were at least operated at 1Hz of sampling frequency to capture rapidly changing concentrations during the passage of a HDT, which is sufficiently fast to measure pollutant concentration peaks (typically 5 to 20 s in duration) as shown in Fig. 1c-e. In general, the duration of a peak was around 5s, for NO_x slightly longer, limiting measurements of high-frequency passages. Euro III HDTs typically emitted a significant amount of PN, PM, NO_x, and non-volatile components (Fig. 1c). More than 95% of Euro III, Euro IV, Euro V, and EEV HDTs had measurable particle emission signals. Significant differences in low particle and gaseous emissions were evident for Euro VI HDTs (Fig. 1d and e).

2.3 Data analysis

The exact time of individual HDTs passing the sampling inlet was determined from the camera recordings and the associated plume pollutant concentrations were integrated to calculate corresponding pollutant emission factors of individual HDTs as described by Hallquist et al. (2013). Emissions of gases and particles from individual HDTs were normalized by the CO_2 concentration to compensate for different degrees of dilution during sampling (Janhäll and Hallquist (2005)). CO_2 peak concentrations exceeding four times the standard deviation of the background signal were used as the base criterion for successful plume capture. Peaks in NO_x, PN, PM, and BC concentrations concurrent with that of CO_2 signify the presence of co-emitted pollutants in a HDT plume. Emission factors (EFs) of gaseous and particle emissions for individual HDTs can then be expressed in units of amount of pollutant emitted per kg fuel burned based on the carbon balance method (Ban-Weiss et al., 2009; Hak et al., 2009):

$$EF_{pollutant} = \frac{\int_{t_1}^{t_2}([pollutant]_t - [pollutant]_{t_1})dt}{\int_{t_1}^{t_2}([CO_2]_t - [CO_2]_{t_1})dt} \times EF_{CO_2} \text{ ,} \tag{1}$$

where $EF_{pollutant}$ is the emission factor of the respective pollutant. The time interval of t_1 to t_2 represents the period when the instruments measured the concentration of an entire pollutant peak from an individual HDT (see Fig. 1c-e). Dallmann et al. (2011) and Preble et al. (2015) used the concepts of inflection points to identify t_1 and t_2. In our study, t_1 and t_2 were determined similarly: t_1 is the point before the pollutant concentration intensity increases abruptly and t_2 is when the intensity becomes relatively flat and undistinguishable compared to background levels. It is noted that the integrated peak intensity is insensitive to the exact location of t_2 since the added integrated signals at or beyond this point are fluctuating around zero. t_1 and t_2 were determined independently of each pollutant peak to account for differences in the time response of individual instruments to the exhaust plume. $\int_{t_1}^{t_2}([pollutant]_t - [pollutant]_{t_1})dt$ and $\int_{t_1}^{t_2}([CO_2]_t - [CO_2]_{t_1})dt$ are the changes in concentration of a pollutant and CO_2 during this time interval. EF_{CO2} of 3158 g (kg diesel fuel)$^{-1}$ was used as the emission factor of CO_2, assuming complete combustion and a carbon content of 86.1% as given in Edwards et al. (2014). Emission factors for plumes with pollutant concentrations lower than our set detection limit (four times the standard deviation of the pollutant background signal) were replaced by the minimum value among all recorded emission factors (EF_{min}) rather than being omitted to avoid inflating emissions from low-emitting HDTs.

3 Results and Discussion

3.1 Fleet compositions

A total of 675 resolved plumes from 556 individual HDTs for the carriage of goods with weights exceeding 12 tonnes were identified. There were 330 Swedish HDTs with Euro type information, 46 Swedish HDTs from which Euro type information was not available, and 180 foreign licensed non-Swedish HDTs. Among the 330 Swedish trucks, Euro III, Euro IV, Euro V, EEV, and Euro VI HDTs accounted for 3%, 5%, 30%, 5%, and 57%, respectively (Fig. S5).

3.2 Emissions variability

Differences in operating and ambient conditions may lead to differences in pollutant emission factors for the same HDT. In this study, we utilized measurement data from 55 HDTs which passed the sampling location repeatedly, yielding a total of 137 plumes. The average pollutant emission factors of each HDT plotted against the individual plume measurements of the corresponding HDT are shown in Fig. S6. In general, the emission factors of PM, non-volatile PN, and NO_x showed little variation ($R^2 \geq 0.77$) among multiple passages of the same HDT, however, higher variability was observed in the PN emissions. This is likely related to variations in the formation of nucleation mode particles from volatile compounds which is more sensitive to driving (Zheng et al., 2014) and dilution conditions. In the following discussion, for HDTs with multiple passages, the average pollutant emission factors of all the detected plumes were used for that individual HDT.

3.3 Emissions factors (EFs) of particles and gaseous pollutants

Figure 2 a and b show the box-and-whisker plots of PM and PN emission factors (EFs) for different Euro classes. Generally, both PM and PN emissions decreased with more stringent Euro emission standards, and especially for Euro VI where larger changes in emission characteristics were evident. These decreasing trends are statistically significant at the 95% CI using the Jonckheere-Terpstra test, a nonparametric test for trends in ordered groups. In addition to PM and PN, the emission trends of BC, NO_x, CO and HC with respect to the level of stringency of Euro standards were statistically examined. Using Euro III HDTs (median EF_{PM}=586 mg (kg fuel)$^{-1}$) as a baseline, the median EF_{PM} for Euro IV, Euro V, EEV, and Euro VI HDTs have been reduced by 78.1%, 86.1%, 88.9%, and 99.8% respectively. In particular, Euro VI HDTs has a median EF_{PM} of only 1.4 mg (kg fuel)$^{-1}$ (Fig. 2a). While it is noted that Euro III to Euro VI standard certifications are based on chassis dynamometer cycle measurements, the Euro VI regulations have started to include additional off-cycle and in-service conformity testing. The Euro emission standard of transient testing for heavy-duty engines gives emission limits as brake specific emission factors, as mass (g) or number (#) of a specific pollutant per kWh. In order to enable a comparison with the Euro emission standard, the EFs in g (or #) per kg fuel were converted using a brake specific fuel consumption (BSFC) of 231.5 g kWh^{-1}. This is the average value for the long haul and regional delivery cycles of chassis dynamometer tests of a typical rigid Euro VI truck (Rexeis et al., 2018). The uncertainty of the BSFC for different Euro class HDTs operating over a wide range of engine conditions is generally within 25% (Mahmoudzadeh Andwari et al., 2017; He et al., 2017; Dreher and Harley, 1998; Heywood, 1988). Note that our measurements represent points of time similar to those in a cycle where the particle emissions can be most prominent. Looking at a whole cycle, this value will be averaged, hence the results from our instantaneous plume measurements may represent an upper limit of the emissions. In Fig. 2a, the right y-axis gives the EFs converted into units of g kWh^{-1} and the Euro standards are shown as blue crosses.

In general, the measured median EF_{PM} are lower than the Euro standards for all HDT types. In particular, the median EF_{PM} for Euro VI HDTs is more than one order of magnitude lower than the Euro standard regulation value since Diesel Particulate Filters (DPFs) are required for these Euro VI HDTs to comply with PM and PN standards (Williams and Minjares, 2016). No information about potential retrofits of tested HDTs was available for the vehicles measured in this study. The effectiveness of DPF in reducing particle emissions have been confirmed by various studies (Martinet et al., 2017; May et al., 2014; Mendoza-Villafuerte et al., 2017; Moody and Tate, 2017; Preble et al., 2015). For example, Bergmann et al. (2009) illustrated that post-DPF PM concentrations decreased by 99.5% compared with pre-DPF for the New European Driving Cycle (NEDC). In real-world measurements, at least ~90% reductions in PM emissions compared to typical pre-DPF levels have been reported (Bishop et al., 2015). Euro emission standards for PM of Euro IV and Euro V heavy-duty diesel engine are the same, while the measured median EF_{PM} of the Euro V fleet was around 1.5 times lower than that of the Euro IV fleet. The control of diesel engine emissions typically requires a compromise between NO_x and particle emission reduction (Clark et al., 1999). The NO_x emission standard is more stringent for Euro V compared to Euro IV (a factor of 43% lower), and hence Euro V HDTs are generally equipped with SCR or EGR to reduce NO_x. In contrast, Euro IV engines are rarely equipped with NO_x after-treatment systems and thus must achieve the NO_x emission limits by tuning the engine performance parameters at the expense of higher PM emissions (Preble et al., 2018; Van Setten et al., 2001). In each of the Euro III, Euro IV, Euro V, and EEV classes, 25-50% of all the measured HDTs had an EF_{PM} higher than their corresponding Euro standards. As described previously, this comparison with the Euro standard is relative and indicative. The higher emissions from individual HDTs may indicate deterioration of engine performance due to wear caused by aging, mileage accumulation, or inadequate maintenance. Our study shows that Euro VI HDTs generally have low PM emissions, but HDTs from older Euro classes frequently exceeded their PM emission limits, suggesting that improved maintenance and suitable retrofitting of older engines are needed.

For PN emissions, EF_{PN} shows an overall trend similar to EF_{PM}. However, large data scatter was evident for Euro VI HDTs, likely due to the sensitivity of nucleation mode particle formation to changes in driving conditions (Fig. 2b). Zheng et al. (2014) reported high concentrations of nucleation mode particles under uphill driving conditions but low concentrations under cruise and downhill driving conditions. It is important to note that the median EF_{PN} of Euro VI HDTs was significantly lower than those from the other Euro type HDTs, which indicates efficient PM removal by the DPF without compromising on total PN emission. Nonetheless, the decrease of particle number in the accumulation mode removes particle surface area available for condensation and therefore favours nucleation of organics from fuel and lubrication oil. Le Breton et al. (2019) confirmed the contribution of lubrication oil in bus emissions. Besides, DPFs can act as a sulphur reservoir and when excess sulphur is released, SO_2 to SO_3 conversion can take place once the after-treatment temperature reaches a critical level (Herner et al., 2011). In this case, total particle number emissions can increase due to nucleation from gas-phase sulphuric acid. Since the fuel sulphur content is low, more than 90% of Euro VI HDTs had an EF_{SO2} lower than the threshold in this study, organics would play a more important role in the formation of nucleation mode particles.

Figure 2c shows that the median EF_{BC} was reduced by more than 99% for Euro VI HDTs compared to Euro III HDTs, and the median EF_{BC} of Euro VI HDTs was even at the threshold (0.2mg (kg fuel)$^{-1}$). The BC emissions generally showed a decrease from Euro III to Euro VI HDTs (Jonckheere-Terpstra test, p<0.01), which is similar to the EF_{PM} trend with the exception of Euro IV HDTs. Compared with Euro V HDTs, the median EF_{BC} of Euro IV HDTs is 35% lower, however, the emission of the mixture of BC and BrC from Euro IV HDTs is higher (Fig. S7a). Euro IV HDTs had the highest BrC contribution to the total light-absorbing substances among all the Euro classes (Fig. S7b).

Figure 2d compares the emissions of NO_2 and NO_x from different Euro class HDTs. The vertical lines represent the different Euro standards. HDTs with either EF_{NO2} or EF_{NOx} lower than the detection limits of the instruments were removed in Fig. 2d for illustration purposes, while all the presented statistical analyse include all the data as outlined above. In general, Euro VI HDTs exhibit more than 90% reduction in both median and average EF_{NOx} compared to Euro III HDTs. This is consistent with Carslaw et al. (2011) who estimated a 93% NO_x reduction from Euro III to Euro VI for heavy goods vehicles

(HGV) in the United Kingdom. Relatively, the Euro V HDTs had a larger fraction exceeding its Euro standard, which may be due to the combined effects of poor engine tuning and the inactivity (low temperature) or deterioration of SCR systems. Newer engines tend to exhibit a higher NO_2 emission fraction at a similar NO_x level, and the Euro VI HDTs show a relatively low median EF_{NO2} with a large range of data scatter and several high emitters. A continuous increase of EF_{NO2}/EF_{NOx} was evident from Euro IV to Euro VI HDTs (Fig. S8b). This trend is consistent with Kozawa et al. (2014), who reported an increase in the share of NO_2 to total NO_x from Euro III to Euro V vehicles. Euro VI HDTs have a higher NO_2 fraction because the DOC upstream of the filter is used to convert NO to NO_2 to control the soot loading in the DPF and facilitate the passive regeneration (Van Setten et al., 2001). A failure of the NO_2 reduction due to the inactivity of the SCR, resulting from low exhaust gas temperature, may result in a higher NO_2 emission (Bishop et al., 2010; Heeb et al., 2010; Herner et al., 2009; May et al., 2014; Thiruvengadam et al., 2015). A more significant decrease in NO_x than NO_2 emissions of Euro VI HDTs may cause an increase of EF_{NO2}/EF_{NOx}.

Table 1 compares the average emission data of PM and PN of the current work with previous studies according to the HDT type and gives information on used measurement methods and driving conditions. Generally, the EF_{PM} and EF_{PN} in this study are within the reported ranges of HDV emissions in the literature. Our estimated EF_{PM} of Euro III HDTs are comparable to those of Euro III buses in Hallquist et al. (2013) and Pirjola et al. (2016). HDTs and buses within the same Euro class emit similar amounts of PM. Watne et al. (2018) show that DPF retrofitted Euro III buses have much lower particle EFs. While EF_{PM} is highly dependent on driving conditions such as speed and acceleration, the average EF_{PM} of Euro IV, Euro V and EEV HDTs of this study:172, 146, and 78 mg (kg fuel)$^{-1}$, respectively, are comparable to trends in previous studies (Hallquist et al., 2013; Pirjola et al., 2016; Watne et al., 2018). Average EF_{PM} of Euro VI HDTs (5 mg (kg fuel)$^{-1}$/ 1.1 mg km^{-1}) is within the range of emissions from HDVs with DPFs, e.g., 0.6 - 20.5 mg km^{-1} for a recent chassis dynamometer test (Jiang et al., 2018) and 2.5 - 8.7 mg km^{-1} for road measurements in California (Quiros et al., 2016). Note that size ranges and measurement methodologies may differ among the studies as listed in Table 1. Since most of the particle emissions related to road traffic combustion are below 560 nm (Fig. 4), the size range in our study is comparable to most other wider range PM measurements. Larger particles from road measurements of total PM may include non-combustion-related particles, e.g. resuspended road dust, tire and brake particles, and should be interpreted with caution. In contrast to EF_{PM}, a much less obvious decrease in average EF_{PN} was observed across different Euro classes. The reason for the high average particle emission for EEV and Euro VI is likely due to high emissions of nucleation mode particles from a number of HDTs.

In Figure 3a, EF_{PM} and EF_{PN} of individual HDTs in this study and selected previous studies are plotted. HDTs with either EF_{PM} or EF_{PN} lower than the detection limits of the instruments (0.07 mg (kg fuel)$^{-1}$ and 2.8×10^{11}# (kg fuel)$^{-1}$ respectively) were removed from the figure (24% of the data) for illustration purposes, while all the presented statistical analyse include all the data as outlined above. Generally, both EF_{PM} and EF_{PN} exhibited a decreasing trend from Euro III to Euro IV and from Euro V to EEV HDTs (Jonckheere-Terpstra test, p<0.01). Overall, Euro VI HDTs had drastically lower PM emissions but highly scattered PN emissions. Older Euro type buses retrofitted with DPF were shown to have reduced particle emissions, and some retrofitted Euro III buses (black open triangles in Fig. 3a) may perform as well as Euro VI HDTs, indicating the effectiveness of retrofitting older HDTs.

In more recent Euro standards, PN regulation has been introduced. The SPN as defined by the European Particle Measurement Program (PMP) is the number of particles which remain after passing through an evaporation tube with a wall temperature of 300-400°C (Zheng et al., 2011). The PMP only measures and regulates solid particles with a diameter larger than 23 nm because measurements of smaller particles in the nucleation mode have poor repeatability (Martini et al., 2009). SPN larger than 23 nm was integrated into the European emission regulation in 2013 for Euro VI heavy-duty engines (Giechaskiel et al., 2012). A potential issue of evaporation measurements is that a fraction of the sub-23 nm particles can also be formed downstream of the European PMP methodology through re-nucleation of semi-volatile precursors (Zheng et al., 2012; Zheng et al., 2011). In our study, the TD temperature of 250ºC is lower than the maximum temperature used by the PMP (300-400ºC) and does not follow the exact operation specifications of the PMP. However, Amanatidis et al. (2018) summarised that TD is a suitable alternative approach for the removal of volatile particles. Particles larger than 23 nm downstream of the TD were measured by the EEPS and we integrated the size bins from 23.5 nm to 560 nm to represent the SPN. Figure 3b compares the EF_{PM} and EF_{SPN} of Euro VI HDTs. Generally, after-treatment control systems could not reduce SPN emissions as effectively as PM emissions, indicating that more control of SPN emission of Euro VI HDTs may be necessary.

Shown in Table 2 are the average EFs of gaseous pollutants (NO_x, CO, HC) in this study compared with other studies. EF_{NOx} generally decreased from the Euro III (43.3 g (kg fuel)$^{-1}$) to Euro VI (3.1 g (kg fuel)$^{-1}$) class, and are in good agreement with reported values for HDTs in the literature. EF_{NOx} of Euro III HDTs is moderately higher in this study. Note that the EF_{NOx} and EF_{PM} of EEV were much higher in Pirjola et al. (2016), in which only a limited number (3-4) vehicles were tested and hard braking was common in approaching a 90° turn before accelerating again. The ratio of EF_{NO2} to EF_{NOx} generally agrees with the projection in Kousoulidou et al. (2008) , on-road plume chasing measurements in Lau et al. (2015) and remote sensing studies in the UK (Carslaw and Rhys-Tyler, 2013). Carslaw et al. (2019) reported a decreasing trend of EF_{NO2}/EF_{NOx} with vehicle mileage for Euro 6 light-duty diesel vehicles, while no significant trend was identified for Euro VI HDTs in this study. There may be other parameters influencing the NO_x emission. For example, Ko et al. (2019) reported that the NO_x emissions from Euro VI diesel vehicles were 29% higher in a traffic jam than in smooth traffic conditions. The temperature of the exhaust and DPF regeneration may also influence the EF_{NOx}.

Compared with EF_{NOx}, EF_{CO} decreased less pronounced from Euro III to Euro VI HDTs (57%). Compared with newer Euro class HDTs, a larger fraction of HDTs in older Euro classes have an EF_{CO} exceeding the Euro standards, which indicates that engine deterioration may have a serious effect on the CO emissions (Fig. S8c). Hallquist et al. (2013) reported a positive relationship between EF_{CO} and EF_{PM}, i.e. high CO indicates incomplete combustion which favors soot formation. DPFs may also reduce CO in addition to PM (Hallquist et al., 2013), which is in agreement with the lowest CO emission of 15.5 g (kg fuel)$^{-1}$observed for DPF equipped Euro VI HDTs in this study. HC emission was relatively low for all HDT types, and no obvious decreasing trend was evident for EF_{HC} from Euro III to Euro VI HDTs (Jonckheere-Terpstra test, p=0.895) (Fig. S8d and Table 2). This does not reflect the more stringent Euro standard limit regarding HC where the Euro VI limit is more than a factor of three lower than the preceding Euro V/IV standards.

The 46 Swedish HDTs without available Euro type information emitted similar levels of particle and gaseous pollutants to Euro VI HDTs and were thus likely equipped with newer Euro engines.

Compared with the fleet of non-Swedish HDTs, the Swedish HDT fleet generally have a lower median and average EF_{NOx} but there are no significant differences in the EF of other pollutants (Fig. 2 and Tables 1 and 2). The differences in EF_{NOx} are significant at the statistical 95% CI using the Kolmogorov-Smirnov test, used in favour to typical student t-test to account for non-normality of the EF distributions. As information of Euro class, engine types and treatment technologies of non-Swedish HDTs is not available, we cannot further explore why there is a difference between the two fleets.

In addition to engine Euro type, pollutant emission trends were also investigated with respect to five different vehicle manufacturers (M1, M2, M3, M4, and M5). EF_{PM}, EF_{PN}, EF_{BC} and EF_{NOx} of HDTs under the same Euro class but from different manufacturers are compared in Fig. S9. Since EF data was not normally distributed, statistical significance is assessed with a Kruskal–Wallis test. It is a non-paramedic analogue of the one-way ANOVA test. The p-values are calculated at the statistical 95% confidence level. No significant group difference (p>0.05) was observed in EF_{PM}, EF_{PN}, $EF_{BC,}$ and EF_{NOx} for Euro V HDTs, i.e., HDTs from five different manufacturers show comparable emission characteristics. EF_{PM}, $EF_{PN,}$ and EF_{NOx} of Euro VI HDTs show no dependency on manufacturers, but a significant difference was observed between M2 and M5 in EF_{BC} of Euro VI HDTs (p=0.016). (No analysis on Euro III, Euro IV, and EEV HDTs was conducted due to the limited vehicle number from each manufacturer).

3.4 Size-resolved EF_{PN} of volatile and non-volatile particles

Figure 4a-e show the average size-resolved number emission factors (solid lines) simultaneously measured via the bypass and TD lines for different Euro class HDTs. The EF_{PN} of the volatile components is calculated as the difference of EF_{PN} measured after the bypass line and the non-volatile component EF_{PN} measured after the TD line. To differentiate between nucleation and accumulation mode particles, a cut point particle diameter of 30 nm was used as defined by Kittelson et al. (2002). In general, all Euro III, Euro IV, Euro V and EEV HDTs showed a bimodal particle number size distribution, with one mode peaking at ~6-10 nm (nucleation mode) and another at ~50-80 nm (accumulation/soot mode) (Maricq, 2007). For Euro VI HDTs the particle number size distributions were dominated by the nucleation mode. The EF_{PN} of the accumulation mode particles shows a decreasing trend from Euro III to EEV HDTs. The accumulation mode of the Euro VI HDTs was insignificant. For heavy-duty diesel engines without a particulate filter, nucleation mode particles are mainly formed from organics. For vehicles with DPF both organics and the fuel sulphur content might influence the formation of nucleation mode particles (Vaaraslahti et al., 2004). Thiruvengadam et al. (2012) found a direct relationship between exhaust nanoparticles in the nucleation mode and the exhaust temperature of the DPF-SCR equipped diesel engine. These factors lead to high variability in the nucleation mode fraction of EF_{PN}. Figure 4f shows that HDVs with DPF (dashed lines) exhibited lower emissions of accumulation mode particles, with no significant reduction in nucleation mode particles when compared to HDVs without DPF (solid lines). In general, the absence of significant accumulation mode particles from Euro VI HDTs was consistent with observations made from DPF equipped HDVs. High emissions of accumulation mode particles from Euro III HDTs were consistent with measurements from HDVs without DPF in previous studies (Liu et al., 2019; Hallquist et al., 2009; Preble et al., 2015).

Most particles in the nucleation mode evaporate after passing through the TD. Sakurai et al. (2003b) reported that volatile compounds in diesel particles are mainly comprised of unburned lubrication oil. The non-volatile components in the nucleation mode may consist of metallic ash from lubrication oil or fuel additives (Sakurai et al., 2003a) or some organic compounds of extremely low volatility (Gkatzelis et al., 2016). In the accumulation mode, the particle mode diameter shifted towards lower sizes after passing the TD. In Fig. 4a-e, we also present the median size distribution (dashed lines). There is a small difference between mean and median size distributions in the accumulation mode while a bigger difference occurs in the nucleation mode. The latter mode is more dynamic and there are larger possibilities for extreme values skewing the averages.

To be consistent with previous studies which overwhelmingly report average size distributions, we choose to utilize the average size distributions for the discussions below. The volatilities of particle emissions in the accumulation and nucleation mode have been evaluated by calculating the average EF_{PN} and EF_{PM} fraction remaining (after heating) of particles emitted from Euro III-VI HDTs (Fig. S10). In general, the EF_{PN} fraction remaining in the nucleation mode was lower than that in the accumulation mode across all HDTs in all Euro classes. In terms of particle mass, the nucleation mode and accumulation mode showed similar EF_{PM} fractions remaining from Euro III to EEV HDTs, while Euro VI HDTs had a much lower EF_{PM} fraction remaining in the nucleation mode than in the accumulation mode. Compared with other Euro class HDTs, Euro VI HDTs had the lowest EF_{PN} and EF_{PM} fraction remaining in both nucleation and accumulation mode. Around 94% of the particles by number and 55% of the particles by mass (or volume) in total were evaporated. Alfoldy et al. (2009) reported that if the same amount of volatile mass in the nucleation mode and accumulation mode were inhaled, 48% and 29% of the mass would deposit in the lung respectively, implying that volatile mass in the nucleation mode would exert a 1.5 times stronger effect.

3.5 Emissions from high emitters

Figure 5 shows the cumulative emission distributions for PM, PN, NO_x, and NO_2 emissions, with HDTs ranked in order from dirtiest to cleanest. The plots show a significant skewedness towards a small fraction of HDTs with a high fraction of total emissions (deviation from 1:1 line) for each pollutant, indicating the importance of "high emitters". The disproportionate skewed distribution of pollutants is a common feature of on-road emission measurements (Preble et al., 2018; Preble et al., 2015; Dallmann et al., 2012). The highest-emitting 10% of HDTs in each pollutant were responsible for 65% of total PM, 70% of total PN, 44% of total NO_x emissions and 69% of total NO_2, respectively. The distribution of NO_x has the least skewedness compared with the other pollutants. If the 10% highest emitters for each pollutant were removed, the corresponding average EF for PM, PN, NO_x, and NO_2 would decrease by 62%, 67%, 38%, and 66% respectively. However, the high emitters for each pollutant are different. For example, Euro III HDTs account for 70% and 67% of the top 3% emitters for PM and BC emissions, while Euro VI HDTs account for 80% and 56% of the top 3% emitters for PN and NO_2 emissions. Here, top 3% emitters were chosen as the reference because Euro III HDTs only accounted for 3% of the total number of HDTs. Lau et al. (Lau et al.,

2015) similarly reported that not all high-emitters were members of the lower Euro classes and that high-emitters for a particular pollutant may not simultaneously be high-emitters for other pollutants.

3.6 Fleet characteristics

Figure 6a-d show the changes in average EFs of PM, PN, BC, and NO_x with respect to the registration year of the HDTs. Triennial average EFs were calculated, with truck registration years divided into 5 bins (2002-2005, 2006-2008, 2009-2011, 2012-2014 and 2015-2017). The black arrows in Fig. 6d show the years that the particular type of HDTs examined in this study was first registered. Coupled with the possible phase-out of older fleets, the HDTs with more advanced engines gradually accounted for a higher proportion of the total fleet. There is a significant improvement during the last years and the transition to widespread adoption of Euro VI will take real-world on-road emissions into a new era of much lower contributions to air pollution.

To estimate for each Euro class the typical contribution of air pollution emissions we utilised the number of kilometres driven by HDTs on Swedish roads. During 2018, 4.1×10^9 and 9.2×10^8 kilometres were driven by Swedish and non-Swedish diesel HDTs on Swedish roads, contributing to 82% and 18% to the total distances travelled by diesel HDTs respectively (Fig. 7a). The numbers of kilometres driven by Swedish Euro 0, Euro I, Euro II, Euro III, Euro IV, Euro V and Euro VI diesel HDTs were 2.8×10^7, 5.0×10^6, 5.4×10^7, 2.0×10^8, 3.1×10^8, 1.3×10^9 and 2.2×10^9 respectively (HBEFA 3.3, 2019). In Figure 7b, the relative contributions of kilometers driven by Swedish Euro 0 to Euro VI HDTs are shown. Zhang et al. (2014) reported no statistically significant difference in fuel consumption among Euro II to Euro IV buses under a real-world typical bus driving cycle in Beijing. In this study, we assume the fuel consumption per kilometre and fuel density are the same across the different Euro class HDTs and adopting the average fuel-based EFs calculated in this study (Tables 1 and 2), the approximation of contributions of pollutants emitted from Swedish HDTs in each Euro class to the total PM, PN, BC and NO_x emissions are depicted in Fig. 7c-f. Due to a lack of corresponding emission information, pollutant average EFs of Euro 0, Euro I and Euro II HDTs were assumed to be at the same level as those of Euro III HDTs representing lower bound estimates. Euro 0-II HDTs accounted for less than 2.2% of the grand total distance driven but totally contributed to 16%, 13%, 6% and 4% of BC, PM, $NO_{x,}$ and PN emissions. Euro III HDTs only accounted for 5% (Fig. 7b) of the total fleet but disproportionally contributed to 37%, 30%, 16% and 10% of BC, PM, $NO_{x,}$ and PN emissions. Euro IV HDTs also exhibited disproportionally high PM and NO_x emissions. A fraction of 32% of HDTs belonged to the Euro V category, they contributed to 53%, 42%, 34%, and 32% of NO_x, PM, BC and PN emissions respectively. Upgrading, replacing or making obsolete Euro 0 to Euro V HDTs would be necessary for mitigating a large part of the PM, PN, BC and NO_x emissions. Euro VI HDTs accounted for the highest fraction of the total fleet (53%), but only contributed to 2%, 6%, 12% and 47% of PM, BC, $NO_{x,}$ and PN emissions, indicating successful overall pollution reduction with the introduction of more Euro VI HDVs. Using the median EFs as references, the emission contributions from Euro VI HDTs to the total pollutant emissions would be even lower (Fig. S11). These data provide useful information to predict future pollutant emission trends and to guide policy analysis and implementation. Since the predicted transition in emissions from road transport would be significant, chemical transport model/cost-assessment models need to get fast access to emission factors for new generation HDTs to be able to provide a better estimation of near future air pollution levels.

4 Atmospheric implications and conclusions

The transition in the atmospheric emission of particles and gases from on-road HDTs caused by the modernisation of the fleet is reported in this study. Particle emissions of PM, BC and to a lesser extent PN exhibited substantial reductions from Euro III to Euro VI HDTs (Jonckheere-Terpstra test, $p<0.01$). The gaseous emissions of NO_x and CO also showed a significant decrease with respect to Euro class (Jonckheere-Terpstra test, $p<0.01$), while the HC emission was relatively low for all the HDT Euro class types. Compared with Euro III HDTs, Euro VI HDTs showed 99%, 98%, 93% and 57% reductions of the average emissions factors of PM, BC, NO_x, and CO respectively. Although a significant reduction in NO_x emissions and a lower median EF_{NO2} were evident, the fraction of NO_2 in the NO_x emissions increased continuously from Euro IV to Euro VI HDTs, and Euro VI HDTs were the dominant class of the top 3% emitters for NO_2. PN showed the largest data scattering for Euro VI HDTs, though after evaporation of the volatile fraction, SPN became less scattered. A plausible reason for this large variability in PN but not PM is the formation of nucleation mode particles containing more volatile compounds, which is more sensitive to individual driving and plume dilution conditions. Reducing particle mass by DPF is clearly important but the consequence in doing so removes particle surface area available for condensation and may therefore favour nucleation mode particle formation if not the precursors of these are also reduced. Furthermore, due to the absence of larger particles, the coagulation rate is decreased and produced nucleation mode particle can retain for a longer time in the atmosphere, which has a direct influence on the evaluation of near-road human exposure.

Driving condition and engine technology affected the size distribution of particle number emissions. The average particle number size distributions of Euro III to EEV HDTs were bimodal with nucleation modes at ~6-10 nm and accumulation modes at ~50-80 nm. Euro VI HDTs displayed nucleation mode dominant size distributions. Measurements of particle volatility revealed that Euro VI HDTs had the highest volatile fraction in both nucleation mode and accumulation mode compared to the other Euro classes. More detailed chemical composition information of this volatile fraction is needed to assess their potential impacts for health and formation of SOA.

We also found that a small number of high emitters contributed to a large fraction of the total emissions. The top 10% emitters in each pollutant category were responsible for 65% of total PM, 70% of total PN, 44% of total NO_x and 69% of total NO_2 emissions, respectively. Euro III HDTs were the dominant top 3% emitters for PM and BC emissions, and Euro VI HDTs were the dominant top 3% emitters for PN and NO_2 emissions.

In general, an overall pollution reduction has been achieved during the last years and the transition to Euro VI adoption will take real-world on-road emissions into a new era of much lower contributions to air pollution. The emissions of PM, BC and NO_x are predicted to further decrease in the future, while PN emissions may be subject to greater fluctuation and therefore be more challenging to control. Upgrading or phasing-out of existing Euro 0 to Euro V vehicles and introducing more Euro VI

HDTs would result in large pollution reductions. More intensive attentions need to be focused on SPN controls for Euro VI HDTs. A careful and more detailed examination of the impacts of fleet upgrades in terms of ambient pollutant levels and emission reduction targets for individual pollutants may be needed for further evaluation.

Data availability.

The data used in this publication are available to the community and can be accessed by request to the corresponding author.

Author contributions.

ÅMH designed the project; LZ, ÅMH, CMS, SMG, ÅS, MJ, HS, MH, and IW conducted the measurements; LZ, CMS, and QL analysed data; LZ, ÅMH, MH, CKC and BPL wrote the paper. All co-authors contributed to the discussion of the manuscript.

Competing interests.

The authors declare that they have no conflict of interest.

Acknowledgments.

This work was financed by Formas (214-2013-1430) and was an initiative within the framework programme "Photochemical smog in China" financed by the Swedish Research Council (639-2013-6917). Chak K. Chan would like to acknowledge the support of the Science Technology and Innovation Committee of Shenzhen Municipality (project no. JCYJ20160401095857424).

References

Alfoldy, B., Giechaskiel, B., Hofmann, W., and Drossinos, Y.: Size-distribution dependent lung deposition of diesel exhaust particles, J. Aerosol Sci., 40, 652-663, 10.1016/j.jaerosci.2009.04.009, 2009.

Amanatidis, S., Ntziachristos, L., Karjalainen, P., Saukko, E., Simonen, P., Kuittinen, N., Aakko-Saksa, P., Timonen, H., Ronkko, T., and Keskinen, J.: Comparative performance of a thermal denuder and a catalytic stripper in sampling laboratory and marine exhaust aerosols, Aerosol Sci. Tech., 52, 420-432, https://doi.org/10.1080/02786826.2017.1422236, 2018.

Arnold, F., Pirjola, L., Ronkko, T., Reichl, U., Schlager, H., Lahde, T., Heikkila, J., and Keskinen, J.: First online measurements of sulfuric acid gas in modern heavy-duty diesel engine exhaust: implications for nanoparticle formation, Environ. Sci. Technol., 46, 11227-11234, https://doi.org/10.1021/es302432s, 2012.

Ban-Weiss, G. A., Lunden, M. M., Kirchstetter, T. W., and Harley, R. A.: Measurement of black carbon and particle number emission factors from individual heavy-duty trucks, Environ. Sci. Technol., 43, 1419-1424, https://doi.org/10.1021/es8021039, 2009.

Bergmann, M., Kirchner, U., Vogt, R., and Benter, T.: On-road and laboratory investigation of low-level PM emissions of a modern diesel particulate filter equipped diesel passenger car, Atmos. Environ., 43, 1908-1916, https://doi.org/10.1016/j.atmosenv.2008.12.039, 2009.

Bishop, G. A., and Stedman, D. H.: A decade of on-road emissions measurements, Environ. Sci. Technol., 42, 1651-1656, https://doi.org/10.1021/es702413b, 2008.

Bishop, G. A., Peddle, A. M., Stedman, D. H., and Zhan, T.: On-road emission measurements of reactive nitrogen compounds from three California cities, Environ. Sci. Technol., 44, 3616-3620, https://doi.org/10.1021/es903722p, 2010.

Bishop, G. A., Schuchmann, B. G., and Stedman, D. H.: Heavy-duty truck emissions in the South Coast Air Basin of California, Environ. Sci. Technol., 47, 9523-9529, https://doi.org/10.1021/es401487b, 2013.

Bishop, G. A., Hottor-Raguindin, R., Stedman, D. H., McClintock, P., Theobald, E., Johnson, J. D., Lee, D. W., Zietsman, J., and Misra, C.: On-road heavy-duty vehicle emissions monitoring system, Environ. Sci. Technol., 49, 1639-1645, https://doi.org/10.1021/es505534e, 2015.

Biswas, S., Verma, V., Schauer, J. J., Cassee, F. R., Cho, A. K., and Sioutas, C.: Oxidative potential of semi-volatile and non-volatile particulate matter (PM) from heavy-duty vehicles retrofitted with emission control technologies, Environ. Sci. Technol., 43, 3905-3912, https://doi.org/10.1021/es9000592, 2009.

Bocchi, C., Bazzini, C., Fontana, F., Pinto, G., Martino, A., and Cassoni, F.: Characterization of urban aerosol: seasonal variation of mutagenicity and genotoxicity of PM2.5, PM1 and semi-volatile organic compounds, Mutat. Res., 809, 16-23, https://doi.org/10.1016/j.mrgentox.2016.07.007, 2016.

Burgard, D. A., Bishop, G. A., Stedman, D. H., Gessner, V. H., and Daeschlein, C.: Remote sensing of in-use heavy-duty diesel trucks, Environ. Sci. Technol., 40, 6938-6942, https://doi.org/10.1021/es060989a, 2006.

Burgard, D. A., and Provinsal, M. N.: On-road, in-use gaseous emission measurements by remote sensing of school buses equipped with diesel oxidation catalysts and diesel particulate filters, J. Air Waste Manag. Assoc., 59, 1468-1473, https://doi.org/10.3155/1047-3289.59.12.1468, 2009.

Campagnolo, D., Cattaneo, A., Corbella, L., Borghi, F., Del Buono, L., Rovelli, S., Spinazze, A., and Cavallo, D. M.: In-vehicle airborne fine and ultra-fine particulate matter exposure: The impact of leading vehicle emissions, Environ. Int., 123, 407-416, https://doi.org/10.1016/j.envint.2018.12.020, 2019.

Carslaw, D. C., Beevers, S. D., Tate, J. E., Westmoreland, E. J., and Williams, M. L.: Recent evidence concerning higher NOx emissions from passenger cars and light-duty vehicles, Atmos. Environ., 45, 7053-7063, https://doi.org/10.1016/j.atmosenv.2011.09.063, 2011.

Carslaw, D. C., and Rhys-Tyler, G.: New insights from comprehensive on-road measurements of NOx, NO2 and NH3 from vehicle emission remote sensing in London, UK, Atmos. Environ., 81, 339-347, https://doi.org/10.1016/j.atmosenv.2013.09.026, 2013.

Carslaw, D. C., Farren, N. J., Vaughan, A. R., Drysdale, W. S., Young, S., and Lee, J. D.: The diminishing importance of nitrogen dioxide emissions from road vehicle exhaust, Atmospheric Environment: X, 1, 100002, https://doi.org/10.1016/j.aeaoa.2018.100002, 2019.

Chen, L., Wang, Z., Liu, S., and Qu, L.: Using a chassis dynamometer to determine the influencing factors for the emissions of Euro VI vehicles, Transport. Res. D- Tr. E., 65, 564-573, https://doi.org/10.1016/j.trd.2018.09.022, 2018.

Cheung, H. H. Y., Tan, H. B., Xu, H. B., Li, F., Wu, C., Yu, J. Z., and Chan, C. K.: Measurements of non-volatile aerosols with a VTDMA and their correlations with carbonaceous aerosols in Guangzhou, China, Atmos. Chem. Phys., 16, 8431-8446, https://doi.org/10.5194/acp-16-8431-2016, 2016.

Clark, N. N., Gautam, M., Rapp, B. L., Lyons, D. W., Graboski, M. S., McCormick, R. L., Alleman, T. L., and Norton, P.: Diesel and CNG transit bus emissions characterization by two chassis dynamometer laboratories: Results and issues, SAE Technical Paper, 0148-7191, 1999.

Cui, M., Chen, Y. J., Feng, Y. L., Li, C., Zheng, J. Y., Tian, C. G., Yan, C. Q., and Zheng, M.: Measurement of PM and its chemical composition in real-world emissions from non-road and on-road diesel vehicles, Atmos. Chem. Phys., 17, 6779-6795, https://doi.org/10.5194/acp-17-6779-2017, 2017.

Dallmann, T. R., DeMartini, S. J., Kirchstetter, T. W., Herndon, S. C., Onasch, T. B., Wood, E. C., and Harley, R. A.: On-road measurement of gas and particle-phase pollutant emission factors for individual heavy-duty diesel trucks, Environ. Sci. Technol., 46, 8511-8518, https://doi.org/10.1021/es301936c, 2012.

Donahue, N. M., Robinson, A. L., Stanier, C. O., and Pandis, S. N.: Coupled partitioning, dilution, and chemical aging of semivolatile organics, Environ. Sci. Technol., 40, 2635-2643, https://doi.org/10.1021/es052297c, 2006.

Dreher, D. B., and Harley, R. A.: A fuel-based inventory for heavy-duty diesel truck emissions, J. Air Waste Manage., 48, 352-358, https://doi.org/10.1080/10473289.1998.10463686, 1998.

Du, Y., Xu, X., Chu, M., Guo, Y., and Wang, J.: Air particulate matter and cardiovascular disease: the epidemiological, biomedical and clinical evidence, J. Thorac. Dis., 8, E8-E19, http://dx.doi.org/10.3978/j.issn.2072-1439.2015.11.37 2016.

Edwards, R., Larivé, J., Rickeard, D., and Weindorf, W.: Well-to-Wheels analysis of future automotive fuels and powertrains in the European context: Well-to-Tank Appendix 2-Version 4a, Joint Research Centre of the European Commission, EUCAR, and CONCAWE, 1-133, http://10.2790/95629, 2014.

EEA: Air Quality in Europe - 2018 Report, 2018.

Franco, V., Kousoulidou, M., Muntean, M., Ntziachristos, L., Hausberger, S., and Dilara, P.: Road vehicle emission factors development: A review, Atmos. Environ., 70, 84-97, https://doi.org/10.1016/j.atmosenv.2013.01.006, 2013.

Gentner, D. R., Jathar, S. H., Gordon, T. D., Bahreini, R., Day, D. A., El Haddad, I., Hayes, P. L., Pieber, S. M., Platt, S. M., de Gouw, J., Goldstein, A. H., Harley, R. A., Jimenez, J. L., Prevot, A. S., and Robinson, A. L.: Review of Urban Secondary Organic Aerosol Formation from Gasoline and Diesel Motor Vehicle Emissions, Environ. Sci. Technol., 51, 1074-1093, https://doi.org/10.1021/acs.est.6b04509, 2017.

Gertler, A. W.: Diesel vs. gasoline emissions: Does PM from diesel or gasoline vehicles dominate in the US?, Atmos. Environ., 39, 2349-2355, https://doi.org/10.1016/j.atmosenv.2004.05.065, 2005.

Giechaskiel, B., Alfoldy, B., and Drossinos, Y.: A metric for health effects studies of diesel exhaust particles, J. Aerosol Sci., 40, 639-651, https://doi.org/10.1016/j.jaerosci.2009.04.008, 2009.

Giechaskiel, B., Mamakos, A., Andersson, J., Dilara, P., Martini, G., Schindler, W., and Bergmann, A.: Measurement of Automotive Nonvolatile Particle Number Emissions within the European Legislative Framework: A Review, Aerosol Sci. Tech., 46, 719-749, https://doi.org/10.1080/02786826.2012.661103, 2012.

Giechaskiel, B., Schwelberger, M., Delacroix, C., Marchetti, M., Feijen, M., Prieger, K., Andersson, S., and Karlsson, H. L.: Experimental assessment of solid particle number Portable Emissions Measurement Systems (PEMS) for heavy-duty vehicles applications, J. Aerosol Sci., 123, 161-170, https://doi.org/10.1016/j.jaerosci.2018.06.014, 2018.

Gkatzelis, G. I., Papanastasiou, D. K., Florou, K., Kaltsonoudis, C., Louvaris, E., and Pandis, S. N.: Measurement of nonvolatile particle number size distribution, Atmos. Meas. Tech., 9, 103-114, https://doi.org/10.5194/amt-9-103-2016, 2016.

Grigoratos, T., Fontaras, G., Giechaskiel, B., and Zacharof, N.: Real-world emissions performance of heavy-duty Euro VI diesel vehicles, Atmos. Environ., 201, 348-359, https://doi.org/10.1016/j.atmosenv.2018.12.042, 2019.

Guo, J. D., Ge, Y. S., Hao, L. J., Tan, J. W., Li, J. Q., and Feng, X. Y.: On-road measurement of regulated pollutants from diesel and CNG buses with urea selective catalytic reduction systems, Atmos. Environ., 99, 1-9, https://doi.org/10.1016/j.atmosenv.2014.07.032, 2014.

Hak, C. S., Hallquist, M., Ljungstrom, E., Svane, M., and Pettersson, J. B. C.: A new approach to in-situ determination of roadside particle emission factors of individual vehicles under conventional driving conditions, Atmos. Environ., 43, 2481-2488, https://doi.org/10.1016/j.atmosenv.2009.01.041, 2009.

Hallquist, A. M., Jerksjo, M., Fallgren, H., Westerlund, J., and Sjodin, A.: Particle and gaseous emissions from individual diesel and CNG buses, Atmos. Chem. Phys., 13, 5337-5350, https://doi.org/10.5194/acp-13-5337-2013, 2013.

Hallquist, M., Wenger, J. C., Baltensperger, U., Rudich, Y., Simpson, D., Claeys, M., Dommen, J., Donahue, N. M., George, C., Goldstein, A. H., Hamilton, J. F., Herrmann, H., Hoffmann, T., Iinuma, Y., Jang, M., Jenkin, M. E., Jimenez, J. L., Kiendler-Scharr, A., Maenhaut, W., McFiggans, G., Mentel, T. F., Monod, A., Prevot, A. S. H., Seinfeld, J. H., Surratt, J. D., Szmigielski, R., and Wildt, J.: The formation, properties and impact of secondary organic aerosol: current and emerging issues, Atmos. Chem. Phys., 9, 5155-5236, https://doi.org/10.5194/acp-9-5155-2009, 2009.

Haugen, M. J., Bishop, G. A., Thiruvengadam, A., and Carder, D. K.: Evaluation of Heavy-and Medium-Duty On-Road Vehicle Emissions in California's South Coast Air Basin, Environ. Sci. Technol., 52, 13298-13305, https://doi.org/10.1021/acs.est.8b03994, 2018.

He, C., Li, J., Ma, Z., Tan, J., and Zhao, L.: High NO2/NOx emissions downstream of the catalytic diesel particulate filter: An influencing factor study, J. Environ. Sci. (China), 35, 55-61, https://doi.org/10.1016/j.jes.2015.02.009, 2015.

He, L., Hu, J., Zhang, S., Wu, Y., Guo, X., Guo, X., Song, J., Zu, L., Zheng, X., and Bao, X.: Investigating real-world emissions of China's heavy-duty diesel trucks: Can SCR effectively mitigate NOx emissions for highway trucks, Aerosol Air. Qual. Res., 17, 2585-2594, https://DOI: 10.4209/aaqr.2016.12.0531, 2017.

Heeb, N. V., Schmid, P., Kohler, M., Gujer, E., Zennegg, M., Wenger, D., Wichser, A., Ulrich, A., Gfeller, U., Honegger, P., Zeyer, K., Emmenegger, L., Petermann, J. L., Czerwinski, J., Mosimann, T., Kasper, M., and Mayer, A.: Impact of low- and high-oxidation diesel particulate filters on genotoxic exhaust constituents, Environ. Sci. Technol., 44, 1078-1084, https://doi.org/10.1021/es9019222, 2010.

Herner, J. D., Hu, S., Robertson, W. H., Huai, T., Collins, J. F., Dwyer, H., and Ayala, A.: Effect of advanced aftertreatment for PM and NO x control on heavy-duty diesel truck emissions, Environ. Sci. Technol., 43, 5928-5933, https://doi.org/10.1021/es9008294, 2009.

Herner, J. D., Hu, S., Robertson, W. H., Huai, T., Chang, M.-C. O., Rieger, P., and Ayala, A.: Effect of advanced aftertreatment for PM and NO x reduction on heavy-duty diesel engine ultrafine particle emissions, Environ. Sci. Technol., 45, 2413-2419, https://doi.org/10.1021/es102792y, 2011.

Heywood, J. B.: Internal combustion engine fundamentals, 1988.

Huffman, J. A., Ziemann, P. J., Jayne, J. T., Worsnop, D. R., and Jimenez, J. L.: Development and characterization of a fast-stepping/scanning thermodenuder for chemically-resolved aerosol volatility measurements, Aerosol Sci. Tech., 42, 395-407, https://doi.org/10.1080/02786820802104981, 2008.

Janhall, S., and Hallquist, M.: A novel method for determination of size-resolved, submicrometer particle traffic emission factors, Environ. Sci. Technol., 39, 7609-7615, https://doi.org/10.1021/es048208y, 2005.

Jarvinen, A., Timonen, H., Karjalainen, P., Bloss, M., Simonen, P., Saarikoski, S., Kuuluvainen, H., Kalliokoski, J., Dal Maso, M., Niemi, J. V., Keskinen, J., and Ronklo, T.: Particle emissions of Euro VI, EEV and retrofitted EEV city buses in real traffic, Environ. Pollut., 250, 708-716, https://doi.org/10.1016/j.envpol.2019.04.033, 2019.

Jiang, Y., Yang, J., Cocker, D., 3rd, Karavalakis, G., Johnson, K. C., and Durbin, T. D.: Characterizing emission rates of regulated pollutants from model year 2012+ heavy-duty diesel vehicles equipped with DPF and SCR systems, Sci. Total Environ., 619-620, 765-771, https://doi.org/10.1016/j.scitotenv.2017.11.120, 2018.

Kittelson, D., Watts, W., and Johnson, J.: Diesel Aerosol Sampling Methodology–CRC E-43, Final report, Coordinating Research Council, 2002.

Ko, J., Myung, C. L., and Park, S.: Impacts of ambient temperature, DPF regeneration, and traffic congestion on NOx emissions from a Euro 6-compliant diesel vehicle equipped with an LNT under real-world driving conditions, Atmos. Environ., 200, 1-14, https://doi.org/10.1016/j.atmosenv.2018.11.029, 2019.

Kousoulidou, M., Ntziachristos, L., Mellios, G., and Samaras, Z.: Road-transport emission projections to 2020 in European urban environments, Atmos. Environ., 42, 7465-7475, https://doi.org/10.1016/j.atmosenv.2008.06.002, 2008.

Kozawa, K. H., Park, S. S., Mara, S. L., and Herner, J. D.: Verifying emission reductions from heavy-duty diesel trucks operating on Southern California freeways, Environ. Sci. Technol., 48, 1475-1483, https://doi.org/10.1021/es4044177, 2014.

Lau, C. F., Rakowska, A., Townsend, T., Brimblecombe, P., Chan, T. L., Yam, Y. S., Mocnik, G., and Ning, Z.: Evaluation of diesel fleet emissions and control policies from plume chasing measurements of on-road vehicles, Atmos. Environ., 122, 171-182, https://doi.org/10.1016/j.atmosenv.2015.09.048, 2015.

Le Breton, M., Psichoudaki, M., Hallquist, M., Watne, Å., Lutz, A., and Hallquist, Å.: Application of a FIGAERO ToF CIMS for on-line characterization of real-world fresh and aged particle emissions from buses, Aerosol Sci. Tech., 1-16, https://doi.org/10.1080/02786826.2019.1566592, 2019.

Lee, B. H., Lopez-Hilfiker, F. D., Mohr, C., Kurten, T., Worsnop, D. R., and Thornton, J. A.: An iodide-adduct high-resolution time-of-flight chemical-ionization mass spectrometer: application to atmospheric inorganic and organic compounds, Environ. Sci. Technol., 48, 6309-6317, https://doi.org/10.1021/es500362a, 2014.

Li, X., Dallmann, T. R., May, A. A., Stanier, C. O., Grieshop, A. P., Lipsky, E. M., Robinson, A. L., and Presto, A. A.: Size distribution of vehicle emitted primary particles measured in a traffic tunnel, Atmos. Environ., 191, 9-18, https://doi.org/10.1016/j.atmosenv.2018.07.052, 2018.

Liu, Q., Hallquist, Å. M., Fallgren, H., Jerksjö, M., Jutterström, S., Salberg, H., Hallquist, M., Le Breton, M., Pei, X., and Pathak, R. K.: Roadside assessment of a modern city bus fleet: Gaseous and particle emissions, Atmospheric Environment: X, 100044, https://doi.org/10.1016/j.aeaoa.2019.100044, 2019.

Liu, Z. G., Vasys, V. N., Dettmann, M. E., Schauer, J. J., Kittelson, D. B., and Swanson, J.: Comparison of Strategies for the Measurement of Mass Emissions from Diesel Engines Emitting Ultra-Low Levels of Particulate Matter, Aerosol Sci. Tech., 43, 1142-1152, https://doi.org/10.1080/02786820903219035, 2009.

Lv, Y., Li, X., Xu, T. T., Cheng, T. T., Yang, X., Chen, J. M., Iinuma, Y., and Herrmann, H.: Size distributions of polycyclic aromatic hydrocarbons in urban atmosphere: sorption mechanism and source contributions to respiratory deposition, Atmos. Chem. Phys., 16, 2971-2983, https://doi.org/10.5194/acp-16-2971-2016, 2016.

Mahmoudzadeh Andwari, A., Pesiridis, A., Esfahanian, V., Salavati-Zadeh, A., Karvountzis-Kontakiotis, A., and Muralidharan, V.: A comparative study of the effect of turbo compounding and ORC waste heat recovery systems on the performance of a turbocharged heavy-duty diesel engine, Energies, 10, 1087, https://doi.org/10.3390/en10081087, 2017.

Manigrasso, M., Vernale, C., and Avino, P.: Traffic aerosol lobar doses deposited in the human respiratory system, Environ. Sci. Pollut. Res. Int., 24, 13866-13873, https://doi.org/10.1007/s11356-015-5666-1, 2017.

Maricq, M. M., and Ning, X.: The effective density and fractal dimension of soot particles from premixed flames and motor vehicle exhaust, J. Aerosol Sci., 35, 1251-1274, https://doi.org/10.1016/j.jaerosci.2004.05.002, 2004.

Maricq, M. M.: Chemical characterization of particulate emissions from diesel engines: A review, J. Aerosol Sci., 38, 1079-1118, https://doi.org/10.1016/j.jaerosci.2007.08.001, 2007.

Martinet, S., Liu, Y., Louis, C., Tassel, P., Perret, P., Chaumond, A., and Andre, M.: Euro 6 Unregulated Pollutant Characterization and Statistical Analysis of After-Treatment Device and Driving-Condition Impact on Recent Passenger-Car Emissions, Environ. Sci. Technol., 51, 5847-5855, https://doi.org/10.1021/acs.est.7b00481, 2017.

Martini, G., Giechaskiel, B., and Dilara, P.: Future European emission standards for vehicles: the importance of the UN-ECE Particle Measurement Programme, Biomarkers, 14 Suppl 1, 29-33, https://doi.org/10.1080/13547500902965393, 2009.

May, A. A., Nguyen, N. T., Presto, A. A., Gordon, T. D., Lipsky, E. M., Karve, M., Gutierrez, A., Robertson, W. H., Zhang, M., Brandow, C., Chang, O., Chen, S. Y., Cicero-Fernandez, P., Dinkins, L., Fuentes, M., Huang, S. M., Ling, R., Long, J., Maddox, C., Massetti, J., McCauley, E., Miguel, A., Na, K., Ong, R., Pang, Y. B., Rieger, P., Sax, T., Truong, T., Vo, T., Chattopadhyay, S., Maldonado, H., Maricq, M. M., and Robinson, A. L.: Gas- and particle-phase primary emissions from in-use, on-road gasoline and diesel vehicles, Atmos. Environ., 88, 247-260, https://doi.org/10.1016/j.atmosenv.2014.01.046, 2014.

Mendoza-Villafuerte, P., Suarez-Bertoa, R., Giechaskiel, B., Riccobono, F., Bulgheroni, C., Astorga, C., and Perujo, A.: NOx, NH3, N2O and PN real driving emissions from a Euro VI heavy-duty vehicle. Impact of regulatory on-road test conditions on emissions, Sci. Total Environ., 609, 546-555, https://doi.org/10.1016/j.scitotenv.2017.07.168, 2017.

Moody, A., and Tate, J.: In Service CO2 and NOX Emissions of Euro 6/VI Cars, Light-and Heavy-dutygoods Vehicles in Real London driving: Taking the Road into the Laboratory, Journal of Earth Sciences and Geotechnical Engineering, 7, 51-62, https://orcid.org/0000-0003-1646-6852, 2017.

Nelson, P. F., Tibbett, A. R., and Day, S. J.: Effects of vehicle type and fuel quality on real-world toxic emissions from diesel vehicles, Atmos. Environ., 42, 5291-5303, https://doi.org/10.1016/j.atmosenv.2008.02.049, 2008.

Pirjola, L., Dittrich, A., Niemi, J. V., Saarikoski, S., Timonen, H., Kuuluvainen, H., Jarvinen, A., Kousa, A., Ronkko, T., and Hillamo, R.: Physical and Chemical Characterization of Real-World Particle Number and Mass Emissions from City Buses in Finland, Environ. Sci. Technol., 50, 294-304, https://doi.org/10.1021/acs.est.5b04105, 2016.

Pirjola, L., Niemi, J. V., Saarikoski, S., Aurela, M., Enroth, J., Carbone, S., Saarnio, K., Kuuluvainen, H., Kousa, A., Ronkko, T., and Hillamo, R.: Physical and chemical characterization of urban winter-time aerosols by mobile measurements in Helsinki, Finland, Atmos. Environ., 158, 60-75, https://doi.org/10.1016/j.atmosenv.2017.03.028, 2017.

Preble, C., Cados, T., Harley, R., and Kirchstetter, T.: Impacts of Aging Emission Control Systems on In-Use Heavy-Duty Diesel Truck Emission Rates, AGU Fall Meeting Abstracts, 2017,

Preble, C. V., Dallmann, T. R., Kreisberg, N. M., Hering, S. V., Harley, R. A., and Kirchstetter, T. W.: Effects of Particle Filters and Selective Catalytic Reduction on Heavy-Duty Diesel Drayage Truck Emissions at the Port of Oakland, Environ. Sci. Technol., 49, 8864-8871, https://doi.org/10.1021/acs.est.5b01117, 2015.

Preble, C. V., Cados, T. E., Harley, R. A., and Kirchstetter, T. W.: In-Use Performance and Durability of Particle Filters on Heavy-Duty Diesel Trucks, Environ. Sci. Technol., 52, 11913-11921, https://doi.org/10.1021/acs.est.8b02977, 2018.

Quiros, D. C., Hu, S. H., Hu, S. S., Lee, E. S., Sardar, S., Wang, X. L., Olfert, J. S., Jung, H. J. S., Zhu, Y. F., and Huai, T.: Particle effective density and mass during steady-state operation of GDI, PFI, and diesel passenger cars, J. Aerosol Sci., 83, 39-54, https://doi.org/10.1016/j.jaerosci.2014.12.004, 2015.

Quiros, D. C., Thiruvengadam, A., Pradhan, S., Besch, M., Thiruvengadam, P., Demirgok, B., Carder, D., Oshinuga, A., Huai, T., and Hu, S.: Real-world emissions from modern heavy-duty diesel, natural gas, and hybrid diesel trucks operating along major California freight corridors, Emission Control Science and Technology, 2, 156-172, https://doi.org/10.1007/s40825-016-0044-0, 2016.

Quiros, D. C., Smith, J. D., Ham, W. A., Robertson, W. H., Huai, T., Ayala, A., and Hu, S.: Deriving fuel-based emission factor thresholds to interpret heavy-duty vehicle roadside plume measurements, J. Air Waste Manag. Assoc., 68, 969-987, https://doi.org/10.1080/10962247.2018.1460637, 2018.

Rexeis, M., Röck, M., and Hausberger, S.: Comparison of Fuel Consumption and Emissions for Representative Heavy-Duty Vehicles in Europe, 2018.

Ristimaki, J., Vaaraslahti, K., Lappi, M., and Keskinen, J.: Hydrocarbon condensation in heavy-duty diesel exhaust, Environ. Sci. Technol., 41, 6397-6402, https://doi.org/10.1021/es0624319, 2007.

Robinson, A. L., Donahue, N. M., Shrivastava, M. K., Weitkamp, E. A., Sage, A. M., Grieshop, A. P., Lane, T. E., Pierce, J. R., and Pandis, S. N.: Rethinking organic aerosols: semivolatile emissions and photochemical aging, Science, 315, 1259-1262, https://doi.org/10.1126/science.1133061, 2007.

Rymaniak, L., Ziolkowski, A., and Gallas, D.: Particle number and particulate mass emissions of heavy-duty vehicles in real operating conditions, MATEC Web of Conferences, 2017, 00025,

Sakurai, H., Park, K., McMurry, P. H., Zarling, D. D., Kittelson, D. B., and Ziemann, P. J.: Size-dependent mixing characteristics of volatile and nonvolatile components in diesel exhaust aerosols, Environ. Sci. Technol., 37, 5487-5495, https://doi.org/10.1021/es034362t, 2003a.

Sakurai, H., Tobias, H. J., Park, K., Zarling, D., Docherty, K. S., Kittelson, D. B., McMurry, P. H., and Ziemann, P. J.: On-line measurements of diesel nanoparticle composition and volatility, Atmos. Environ., 37, 1199-1210, https://doi.org/10.1016/S1352-2310(02)01017-8, 2003b.

Smit, R., Keramydas, C., Ntziachristos, L., Lo, T. S., Ng, K. L., Wong, H. L. A., and Wong, C.: Evaluation of real-world gaseous emissions performance of SCR and DPF bus retrofits, Environ. Sci. Technol., https://doi.org/10.1021/acs.est.8b07223, 2019.

Tan, Y., Henderick, P., Yoon, S., Herner, J., Montes, T., Boriboonsomsin, K., Johnson, K., Scora, G., Sandez, D., and Durbin, T. D.: On-Board Sensor-Based NOx Emissions from Heavy-Duty Diesel Vehicles, Environ. Sci. Technol., 53, 5504-5511, https://doi.org/10.1021/acs.est.8b07048, 2019.

Thiruvengadam, A., Besch, M. C., Carder, D. K., Oshinuga, A., and Gautam, M.: Influence of real-world engine load conditions on nanoparticle emissions from a DPF and SCR equipped heavy-duty diesel engine, Environ. Sci. Technol., 46, 1907-1913, https://doi.org/10.1021/es203079n, 2012.

Thiruvengadam, A., Besch, M. C., Thiruvengadam, P., Pradhan, S., Carder, D., Kappanna, H., Gautam, M., Oshinuga, A., Hogo, H., and Miyasato, M.: Emission rates of regulated pollutants from current technology heavy-duty diesel and natural gas goods movement vehicles, Environ. Sci. Technol., 49, 5236-5244, https://doi.org/10.1021/acs.est.5b00943, 2015.

Vaaraslahti, K., Virtanen, A., Ristimaki, J., and Keskinen, J.: Nucleation mode formation in heavy-duty diesel exhaust with and without a particulate filter, Environ. Sci. Technol., 38, 4884-4890, https://doi.org/10.1021/es0353255, 2004.

Van Setten, B. A., Makkee, M., and Moulijn, J. A.: Science and technology of catalytic diesel particulate filters, Catalysis Reviews, 43, 489-564, https://doi.org/10.1081/CR-120001810, 2001.

Vojtisek-Lom, M., Pechout, M., Dittrich, L., Beranek, V., Kotek, M., Schwarz, J., Vodicka, P., Milcova, A., Rossnerova, A., Ambroz, A., and Topinka, J.: Polycyclic aromatic hydrocarbons (PAH) and their genotoxicity in exhaust emissions from a diesel engine during extended low-load operation on diesel and biodiesel fuels, Atmos. Environ., 109, 9-18, https://doi.org/10.1016/j.atmosenv.2015.02.077, 2015.

Wang, T., Quiros, D. C., Thiruvengadam, A., Pradhan, S., Hu, S., Huai, T., Lee, E. S., and Zhu, Y.: Total Particle Number Emissions from Modern Diesel, Natural Gas, and Hybrid Heavy-Duty Vehicles During On-Road Operation, Environ. Sci. Technol., 51, 6990-6998, https://doi.org/10.1021/acs.est.6b06464, 2017.

Watne, A. K., Psichoudaki, M., Ljungstrom, E., Le Breton, M., Hallquist, M., Jerksjo, M., Fallgren, H., Jutterstrom, S., and Hallquist, A. M.: Fresh and Oxidized Emissions from In-Use Transit Buses Running on Diesel, Biodiesel, and CNG, Environ. Sci. Technol., 52, 7720-7728, https://doi.org/10.1021/acs.est.8b01394, 2018.

Williams, M., and Minjares, R.: A technical summary of Euro 6/VI vehicle emission standards, International Council for Clean Transportation (ICCT), Washington, DC, accessed July, 10, 2017, 2016.

Zavala, M., Molina, L. T., Yacovitch, T. I., Fortner, E. C., Roscioli, J. R., Floerchinger, C., Herndon, S. C., Kolb, C. E., Knighton, W. B., Paramo, V. H., Zirath, S., Mejia, J. A., and Jazcilevich, A.: Emission factors of black carbon and co-pollutants from diesel vehicles in Mexico City, Atmos. Chem. Phys., 17, 15293-15305, https://doi.org/10.5194/acp-17-15293-2017, 2017.

Zhang, S. J., Wu, Y., Liu, H., Huang, R. K., Yang, L. H. Z., Li, Z. H., Fu, L. X., and Hao, J. M.: Real-world fuel consumption and CO2 emissions of urban public buses in Beijing, Appl. Energ., 113, 1645-1655, https://doi.org/10.1016/j.apenergy.2013.09.017, 2014.

Zheng, Z., Johnson, K. C., Liu, Z., Durbin, T. D., Hu, S., Huai, T., Kittelson, D. B., and Jung, H. S.: Investigation of solid particle number measurement: Existence and nature of sub-23 nm particles under PMP methodology, J. Aerosol Sci., 42, 883-897, https://doi.org/10.1016/j.jaerosci.2011.08.003, 2011.

Zheng, Z., Durbin, T. D., Xue, J., Johnson, K. C., Li, Y., Hu, S., Huai, T., Ayala, A., Kittelson, D. B., and Jung, H. S.: Comparison of particle mass and solid particle number (SPN) emissions from a heavy-duty diesel vehicle under on-road driving conditions and a standard testing cycle, Environ. Sci. Technol., 48, 1779-1786, https://doi.org/10.1021/es403578b, 2014.

Zheng, Z. Q., Durbin, T. D., Karavalakis, G., Johnson, K. C., Chaudhary, A., Cocker, D. R., Herner, J. D., Robertson, W. H., Huai, T., Ayala, A., Kittelson, D. B., and Jung, H. S.: Nature of Sub-23-nm Particles Downstream of the European Particle Measurement Programme (PMP)-Compliant System: A Real-Time Data Perspective, Aerosol Sci. Tech., 46, 886-896, https://doi.org/10.1080/02786826.2012.679167, 2012.

Zhu, Y. F., Hinds, W. C., Kim, S., Shen, S., and Sioutas, C.: Study of ultrafine particles near a major highway with heavy-duty diesel traffic, Atmos. Environ., 36, 4323-4335, https://doi.org/10.1016/S1352-2310(02)00354-0, 2002.

Table 1. Comparison of the average emission data[a] for PM and PN from the present study with literature data.

PM/PN						
Vehicle type	Speed km h^{-1}	Dp range nm	Method	Instrument	EF_{PM} mg (kg fuel)$^{-1}$	EF_{PN} # (kg fuel)$^{-1}$ 10^{14}
Euro III HDT in this study	26±6[b]	5.6-560	roadside	EEPS	684±365	20.3±11.7
Euro III bus (Hallquist et al., 2013)	acceleration	5.6-560	roadside	EEPS	6.7-2074	0.11-45
	constant speed	5.6-560	roadside	EEPS	151-273	0.12-4.2
Euro III bus with DPF (Hallquist et al., 2013)	acceleration	5.6-560	roadside	EEPS	62-2465	1.9-23
	constant speed	5.6-560	roadside	EEPS	41-142	1.1-9.7
Euro III bus (Pirjola et al., 2016)	≤25 (bus depot)	PM_1 D_p ≥2.5	plume chasing	ELPI[c] CPC	1240±220[b]	20.6±3.2[b]
	≤45 (bus line)	PM_1 D_p ≥2.5	plume chasing	ELPI[c] CPC	500	17.7
Euro III bus with DPF+SCR (Watne et al., 2018)	acceleration	5.6-560	roadside	EEPS	8.9±0.2	0.12±0.12
Euro III bus with DPF+SCR (Liu et al., 2019)	stop and go (bus stop)	5.6-560	roadside	EEPS	30±26[b]	14.0±3.0[b]
Euro III diesel bus and truck (Zavala et al., 2017)	driving cycle	35-1000	plume chasing & roadside	SP-AMS[f]	4300	-
Euro IV HDT in this study	23±8[b]	5.6-560	roadside	EEPS	172±68	8.7±3.0
Euro IV bus with EGR (Hallquist et al., 2013)	acceleration	5.6-560	roadside	EEPS	562-3089	13-44
	constant speed	5.6-560	roadside	EEPS	91-489	5.8-47
Euro IV bus with EGR+DPF (Hallquist et al., 2013)	acceleration	5.6-560	roadside	EEPS	177-650	5.1-13
	constant speed	5.6-560	roadside	EEPS	58-61	2.6-3.1
Euro IV bus with EGR+DPF (Pirjola et al., 2016)	≤25 (bus depot)	PM_1 D_p ≥2.5	plume chasing	ELPI[c] CPC	1190±520[b]	8.9±1.6[b]
Euro IV bus with SCR (Watne et al., 2018)	acceleration	5.6-560	roadside	EEPS	145-560	3-13
Euro IV diesel bus and truck (Zavala et al., 2017)	driving cycle	35-1000	plume chasing and roadside	SP-AMS[f]	1800	-
Euro V HDT in this study	27±7[b]	5.6-560	roadside	EEPS	146±49	9.7±2.7
Euro V bus+SCR (Hallquist et al., 2013)	acceleration	5.6-560	roadside	EEPS	125-766	4.4-92
	constant speed	5.6-560	roadside	EEPS	41-509	2.7-33
Euro V bus (Watne et al., 2018)	acceleration	5.6-560	roadside	EEPS	145±70	3.0±1.7
Euro V HDV with SCR (Rymaniak et al., 2017)	average at 45	PM/ 5.6-560	PEMS	MSS[e] EEPS	1840 [d]	0.09 [d]
Euro V bus with SCR (Liu et al., 2019)	stop and go (bus stop)	5.6-560	roadside	EEPS	180±15[b]	6.5±2.9[b]
Euro V diesel bus and truck (Zavala et al., 2017)	driving cycle	35-1000	plume chasing and roadside	SP-AMS[f]	720	-
EEV HDT in this study	25±8[b]	5.6-560	roadside	EEPS	78±35	16.5±23.6

EEV bus with EGR +DPF (Pirjola et al., 2016)	≤25 (bus depot)	PM_1/ $D_p \geq 2.5$	plume chasing	ELPI[c] CPC	400±280[b]	2.1±0.1[b]
EEV bus with SCR (Pirjola et al., 2016)	≤25 (bus depot)	PM_1/ $D_p \geq 2.5$	plume chasing	ELPI[c] CPC	280±170[b]	7.0±3.8[b]
EEV with DOC+DPF+SCR (Rymaniak et al., 2017)	average at 45	PM/ 5.6-560	PEMS	MSS[e] EEPS	236 [d]	0.02 [d]
EEV bus (Jarvinen et al., 2019)	stop and go	PM_1/ $D_p \geq 3$	plume chasing	ELPI[c] CPC	200	8.6
Euro VI HDT in this study	29±8[b]	5.6-560	roadside	EEPS	5±2	8.5±4.6
Euro VI bus (Jarvinen et al., 2019)	stop and go	PM_1/ $D_p \geq 3$	plume chasing	ELPI[c] CPC	70	5
Euro VI HDGV (Moody and Tate, 2017)	13-86	-	PEMS	-	28-33[d]	-
Euro VI HDT (Grigoratos et al., 2019)	65-74	-	PEMS	-	-	0.002-0.01[d]
HDT without available Euro type information	27±7[b]	5.6-560	roadside	EEPS	47±23	7.5±7.3
Total Swedish HDT	28±7[b]	5.6-560	roadside	EEPS	96±36	9.6±2.7
Total non-Swedish HDT	26±8[b]	5.6-560	roadside	EEPS	117±42	11.1±4.2
Non-European HDV with different ATS						
HDV with DPF (Wang et al., 2017; Quiros et al., 2016)	13-80	PM $D_p \geq 5$	PEMS	gravimetric CPC	12-41[d]	0.006-13.2
Heavy-duty HDV with DPF+SCR (Thiruvengadam et al., 2015)	driving cycle	PM	chassis dynamometer	gravimetric	6-29 [d]	-
HDV with DPF+SCR (Jiang et al., 2018)	driving cycle	$PM_{2.5}$	chassis dynamometer	gravimetric	3-97 [d]	-
HDT (model year 2004- 2006) (Preble et al., 2015)	accelerating or cruise at 48	$D_p \geq 2.5$	roadside	CPC	-	47.2±9.7
HDT with SCR+DPF (model year 2010- 2013) (Preble et al., 2015)		$D_p \geq 2.5$	roadside	CPC	-	15.9±11.5
HDV (mean model year 2005) (Bishop et al., 2015)	15.7-16.8	$PM_{1.2}$	OHMS[g]	digital mass monitor	650	-
HDV (mean model year 2009) (Bishop et al., 2015)	7.7-9.3	$PM_{1.2}$	OHMS[g]	digital mass monitor	31	-
HDV without after-treatment (Quiros et al., 2018)	driving cycle	$PM_{2.5}$	chassis dynamometer	gravimetric	1980[d]	-
HDV+DPF (Quiros et al., 2018)	driving cycle	$PM_{2.5}$	chassis dynamometer	gravimetric	6-9[d]	-

[a] Given errors are at 95% CI.
[b] Standard deviation.
[c] ELPI, Electrical Low-Pressure Impactor.

[d] Average fuel consumption of 0.26 L km^{-1} for HDV during long haul and regional delivery tests (Rexeis et al., 2018), the density of 0.815 kg dm^{-3} (Swedish Environmental Protection Agency, 2013) of diesel particles were assumed for unit conversion.

[e] MSS, Micro Soot Sensor.

[f] SP-AMS, Soot Particle Aerosol Mass Spectrometer.

[g] OHMS, On-Road Heavy-Duty Vehicle Emissions Monitoring System.

Table 2. Comparison of the average emission data[a] for NO_x, NO_2/NO_x, CO and HC from the present study with literature data.

Vehicle type	Speed km h^{-1}	Method	EF_{NO_x}[b] g (kg fuel)$^{-1}$	EF_{NO_2}/ EF_{NO_x}[b] mass ratio %	EF_{CO}[c] g (kg fuel)$^{-1}$	EF_{HC}[c] g (kg fuel)$^{-1}$
Euro III HDT in this study	26±6[d]	roadside	43.3±31.5	7.5±4.1	36.0±13.2	0.8±1.3
Euro III bus (Hallquist et al., 2013)	acceleration	roadside	16.1±9.7	-	16.1±16.1	<13
Euro III bus (Pirjola et al., 2016)	≤25 (bus depot)	plume chasing	12.7±1.8[d]	-	-	-
	≤45 (bus line)	plume chasing	20.5	-	-	-
Euro III bus with DPF+SCR (Watne et al., 2018)	acceleration	roadside	-	-	13±10	0.02
Euro III HDV (Lau et al., 2015)	64 ± 13[d]	plume chasing	-	24±4	-	-
Euro III &IV HDV (Kousoulidou et al., 2008)	-	model	-	14	-	-
Euro III HGV (Carslaw et al., 2011)	Average at 31	remote sensing	16.2±1.0[f]	-	-	-
Euro III HGV (Carslaw and Rhys-Tyler, 2013)	28-60	remote sensing	-	24.1±4.7	-	-
Euro IV HDT in this study	23±8[d]	roadside	19.8±10.1	2.7±2.9	22.1±10.3	0.7±1.1
Euro IV bus (Hallquist et al., 2013)	acceleration	roadside	12.9±6.5	-	16.1±16.1	<13
Euro IV bus with EGR+DPF (Pirjola et al., 2016)	≤25 (bus depot)	plume chasing	23.4±6.1[d]	-	-	-
Euro IV bus with SCR (Watne et al., 2018)	roadside	acceleration	-	-	220-230	0.3-0.6
Euro IV HDV (Lau et al., 2015)	64 ± 13[d]	plume chasing	-	28±5	-	-
Euro IV HGV (Carslaw et al., 2011)	average at 31	remote sensing	10.3±1.4[f]	-	-	-
Euro IV HGV (Carslaw and Rhys-Tyler, 2013)	28-60	remote sensing	-	3.1±0.7	-	-
Euro V HDT in this study	27±7[d]	roadside	22.2±3.8	6.0±2.8	22.8±5.1	0.9±0.4
Euro V bus (Hallquist et al., 2013)	acceleration	roadside	35.5±9.7	-	9.7±3.2	<13
Euro V bus with SCR (Liu et al., 2019)	stop and go (bus stop)	roadside	9.8±3.5[d]	3.7±1.5[d]	28[e]	2.2[e]
Euro V HDV (Lau et al., 2015)	64 ± 13[d]	plume chasing	-	40±14	-	-
Euro V HDV (Kousoulidou et al., 2008)	-	model	-	18	-	-
Euro V HGV (Carslaw et al., 2011)	average at 31	remote sensing	13.3±5.8[f]	-	-	-
Euro V HGV (Carslaw and Rhys-Tyler, 2013)	28-60	remote sensing	-	3.7±0.7	-	-

EEV HDT in this study	25±8[d]	roadside	13.6±6.7	6.3±3.7	18.0±10.1	0.2±0.4
EEV bus with EGR +DPF (Pirjola et al., 2016)	≤25 (bus depot)	plume chasing	32.9±7.6[d]	-	-	-
EEV bus with SCR (Pirjola et al., 2016)	≤25 (bus depot)	plume chasing	39.8±4.2[d]	-	-	-
Euro VI HDT in this study	29±8[d]	roadside	3.1±1.0	22.5±4.2	15.5±2.2	1.0±0.5
Euro VI HDT (Grigoratos et al., 2019)	65-74	PEMS	0.3-31.3	-	2.8-22.3	0.3-3.1
Euro VI HDV (Kousoulidou et al., 2008)	-	model	-	35	-	-
Euro VI HDV (Moody and Tate, 2017)	driving cycle	PEMS	2.2[f]	-	-	-
HDT without available Euro type information	27±7[d]	roadside	7.8±4.5	13.9±6.3	20.7±5.6	0.8±0.6
Total Swedish HDT	28±7[d]	roadside	10.7±1.8	15.9±2.5	18.6±1.9	0.9±0.3
Total non-Swedish HDT	26±8[d]	roadside	13.0±2.5	12.7±3.0	19.1±3.0	0.9±0.6
Non-European HDV with different ATS						
Heavy-duty HDV with DPF+SCR (Thiruvengadam et al., 2015)	driving cycle	chassis dynamometer	3.8-27.8[f]	-	0.1-13.4 [f]	<0.64 [f]
HDV with DPF+SCR (Jiang et al., 2018)	driving cycle	chassis dynamometer	0.2-66.4[f]	-	0.006-14.9[f]	<1.3 [f]
HDV with DOC+DPF+SCR (Quiros et al., 2016)	12.7-85.6	mobile laboratory	1.7-11.8[f]	-	0.9-2.8 [f]	0.1-0.4 [f]
HDV (May et al., 2014)	driving cycle	chassis dynamometer	30-43	-	-	-
HDV with SCR (May et al., 2014)		chassis dynamometer	11	-	-	-
HDV fleet average (Haugen et al., 2018)	22.5±0.9	remote sensing	12.4±0.6	8.9	5.9±0.9	2.2±0.4
HDT (model year 2004- 2006) (Preble et al., 2015)	accelerating or cruise at 48	roadside	16.5±1.7	3.4±1.8	-	-
HDT with SCR+DPF (model year 2010- 2013) (Preble et al., 2015)		roadside	5.1±1.2	22.1±8.4	-	-
HDT (model year 2001) (Burgard et al., 2006)	5-25	roadside	-	9.1±0.5	26.0±2.1	1.8±0.6
HDT (model year 2000) (Burgard et al., 2006)	20-40	roadside	-	6.1±0.1	37.9±1.6	3.3±0.4
Fleet average in 2006 (Bishop and Stedman, 2008)	28-36	roadside	2-5	-	17-24	1.9-2.3
HDT fleet average (Dallmann et al., 2012)	65	roadside	28±1.5	7.0	8.0±1.2	-
HDT (mean model year 2004) (Bishop et al., 2013)	22.2±0.4	remote sensing	20.6±0.6[d]	9.7	8.2±0.6 [d]	3.7±0.1 [d]

HDT (mean model year 2009) (Bishop et al., 2013)	7.8±0.1	remote sensing	19.9±0.3 [d]	9.0	7.3±0.5 [d]	0.6±0.6 [d]

[a] Given errors are at 95% CI.
[b] In NO_2 equivalents.
[c] RSD data. For the RSD data sets of multiple individuals, negative values were replaced by zero when calculating the averages.
[d] Standard deviation.
[e] Median.
[f] Average fuel consumption of 0.26 L km^{-1} for HDV during long haul and regional delivery tests (Rexeis et al., 2018), the density of 0.815 kg dm^{-3} (Swedish Environmental Protection Agency, 2013) of diesel particles were assumed.

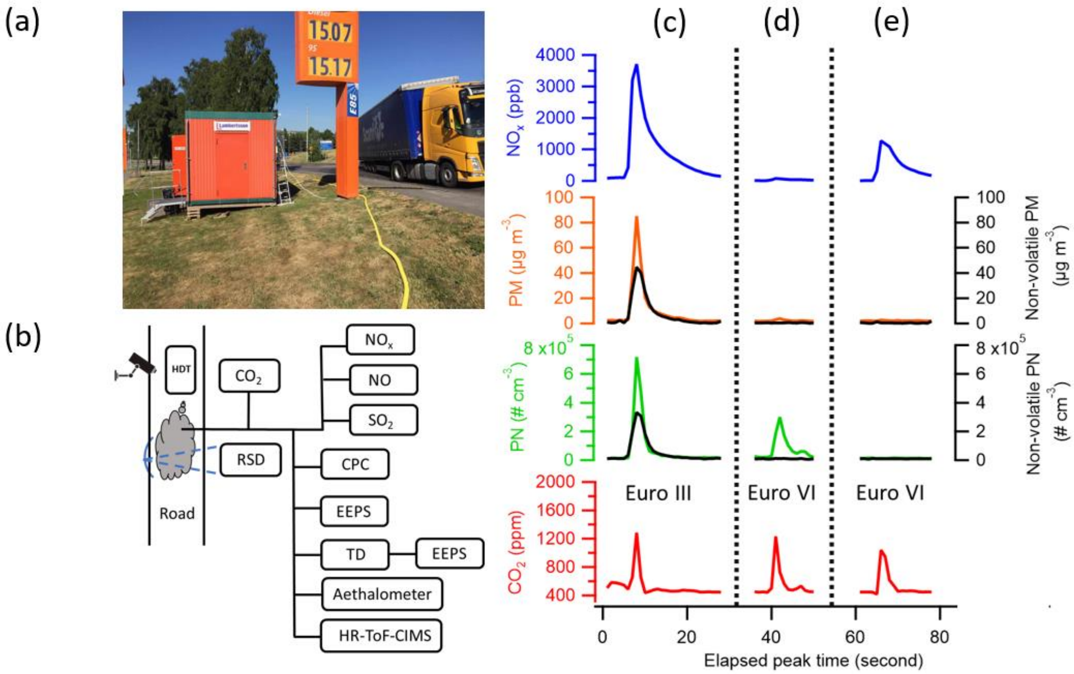

Figure 1. (a) Sampling site at the roadside in Gothenburg, Sweden, (b) schematic of the experimental set-up. HDT (Heavy-duty truck), RSD (Remote Sensing Device), CPC (Condensation Particle Counter), EEPS (Engine Exhaust Particle Sizer Spectrometer), TD (Thermodenuder) and HR-ToF-CIMS* (High-Resolution Time-of-Flight Chemical Ionization Mass Spectrometer) and examples of signals from three passing HDTs. Concentrations of CO_2, PN, non-volatile PN (black line), PM, non-volatile PM (black line), and NO_x from (c) a typical Euro III HDT and (d) a typical Euro VI HDT and (e) a Euro VI HDT with low PN emission. *The data from the HR-ToF-CIMS will be presented elsewhere.

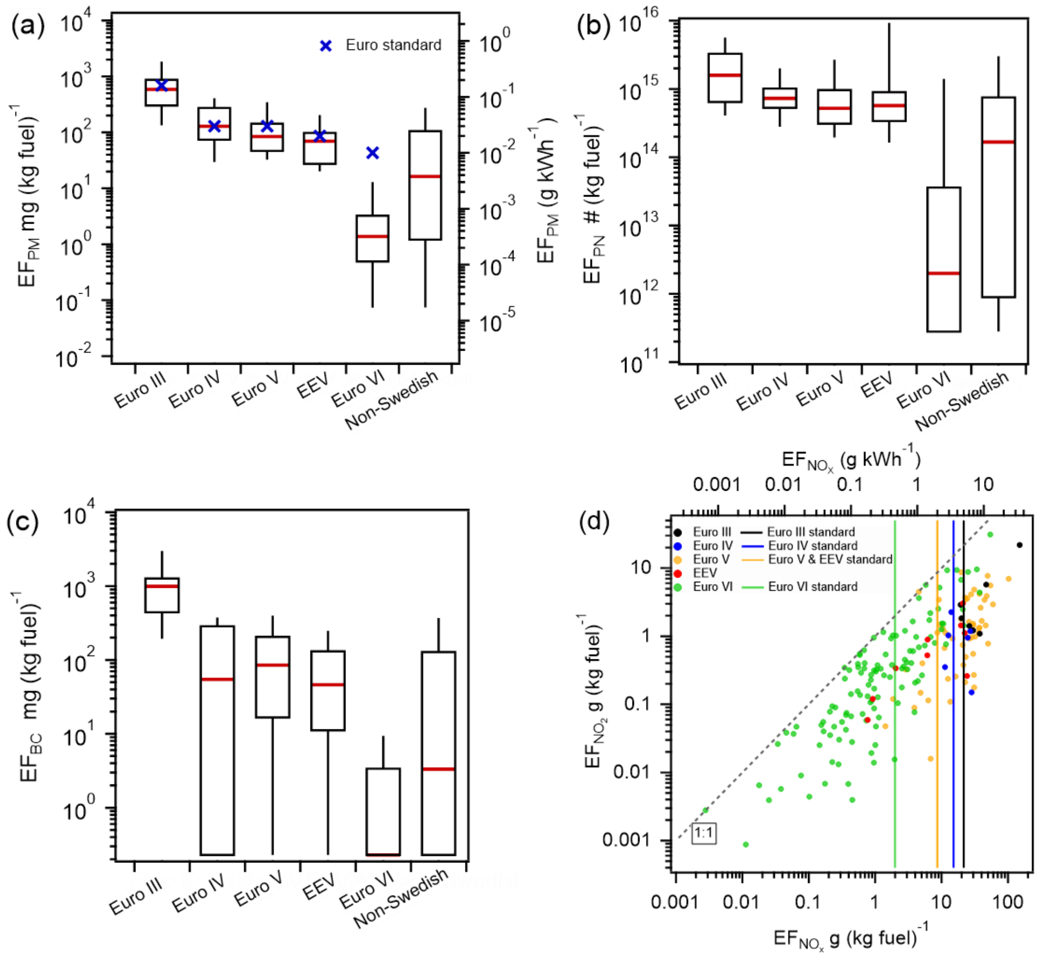

Figure 2. (a) EF_{PM}, (b) EF_{PN}, (c) EF_{BC}, (d) EF_{NO2} and EF_{NOx} for Euro III to Euro VI and non-Swedish HDTs. Non-detectable pollutant emission signals for captured plumes have been replaced by EF_{min}. For box-and-whisker plots, the top and the bottom line of the box are 75th and 25th percentiles of the data, the red line inside the box is the median, and the top and bottom whiskers are 90th and 10th percentiles. EF_{NOx} in (d) are in NO_2 equivalents. HDTs with either EF_{NO2} or EF_{NOx} lower than the detection limits of the instruments were removed in (d) for illustration purposes. Note that the comparison with the emission standard is only indicative as they are based on test cycle performance.

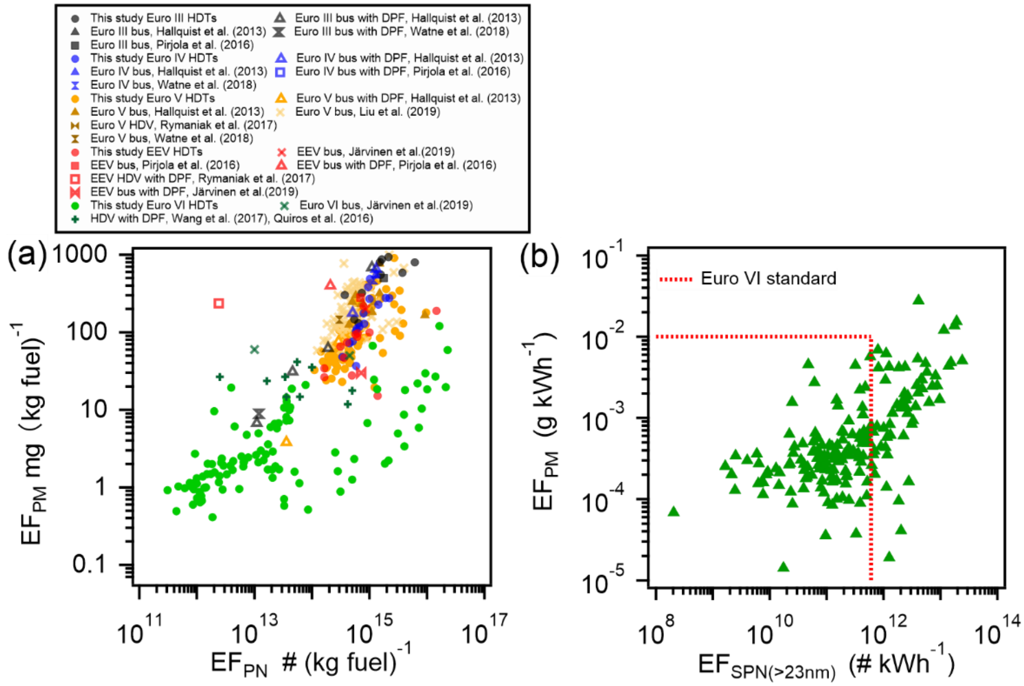

Figure 3. (a) EF_{PM} and EF_{PN} of individual HDTs in this study and previous studies and (b) the relationship between EF_{PM} and EF_{SPN} of Euro VI HDTs. Red dashed lines represent Euro emission standards (horizontal: PM emission standard; vertical: SPN emission standard). HDTs with either EF_{PM} or EF_{PN} lower than the detection limits of the instruments were removed in (a) for illustration purposes. Note that the comparison with the emission standard is only indicative as they are based on test cycle performance.

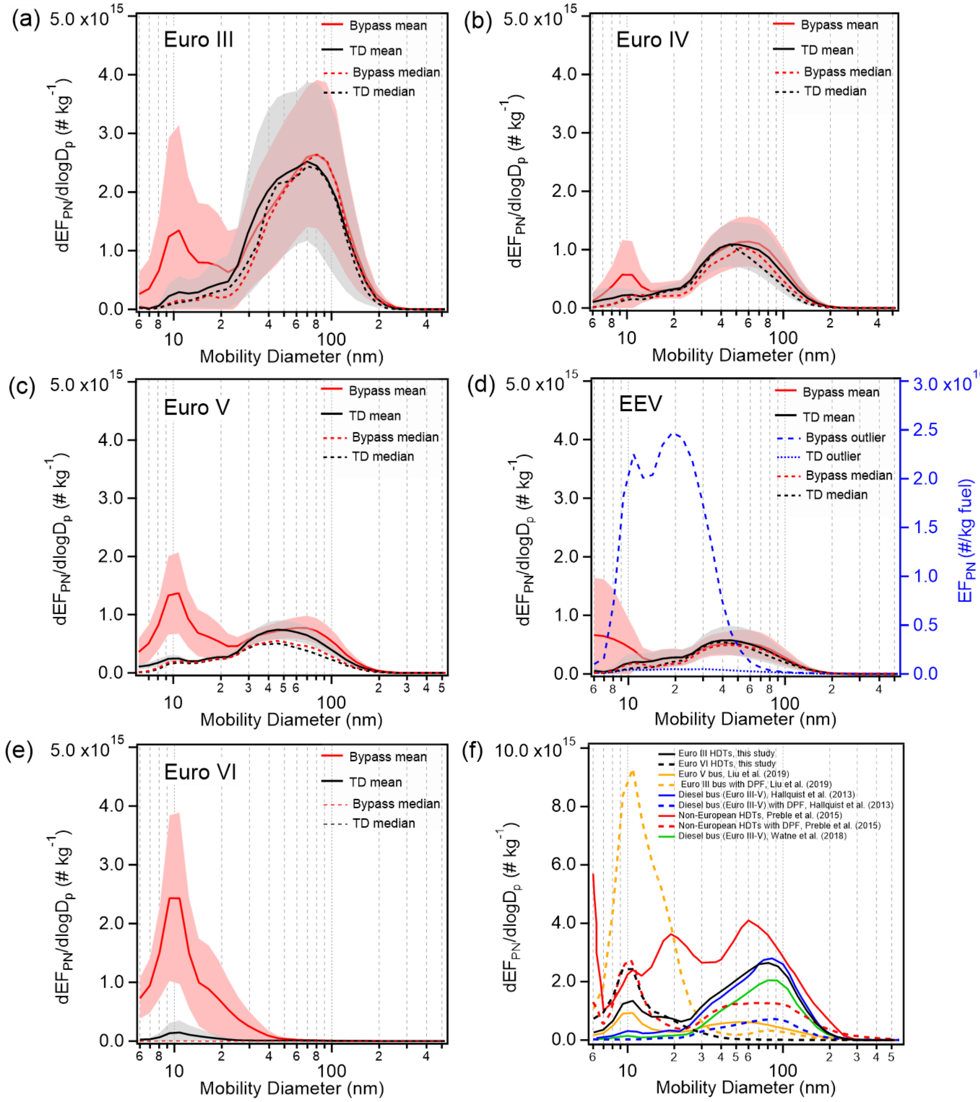

Figure 4. (a-e) Mean and median size-resolved EF_{PN} and $EF_{non\text{-}volatile\ PN}$ of different Euro class HDTs and (f) comparisons of mean size-resolved EF_{PN} of HDVs in this study and previous studies. Shaded regions in (a-e) represent the statistical 95% confidence interval. One HDT with extremely different EF in (d) was excluded and shown in blue.

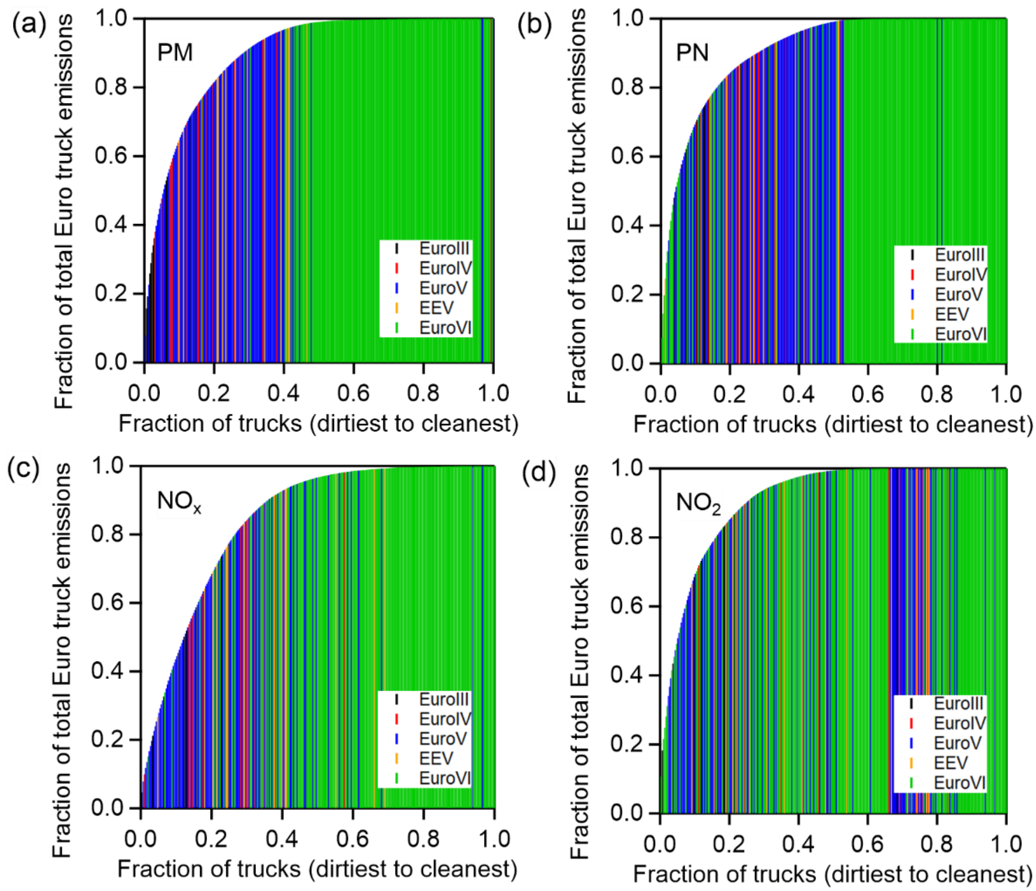

Figure 5. Cumulative emission factor distribution for (a) PM, (b) PN, (c) NO_x, and (d) NO_2 measured in HDT exhaust plumes with HDTs ranked from the highest to lowest in terms of emission factors.

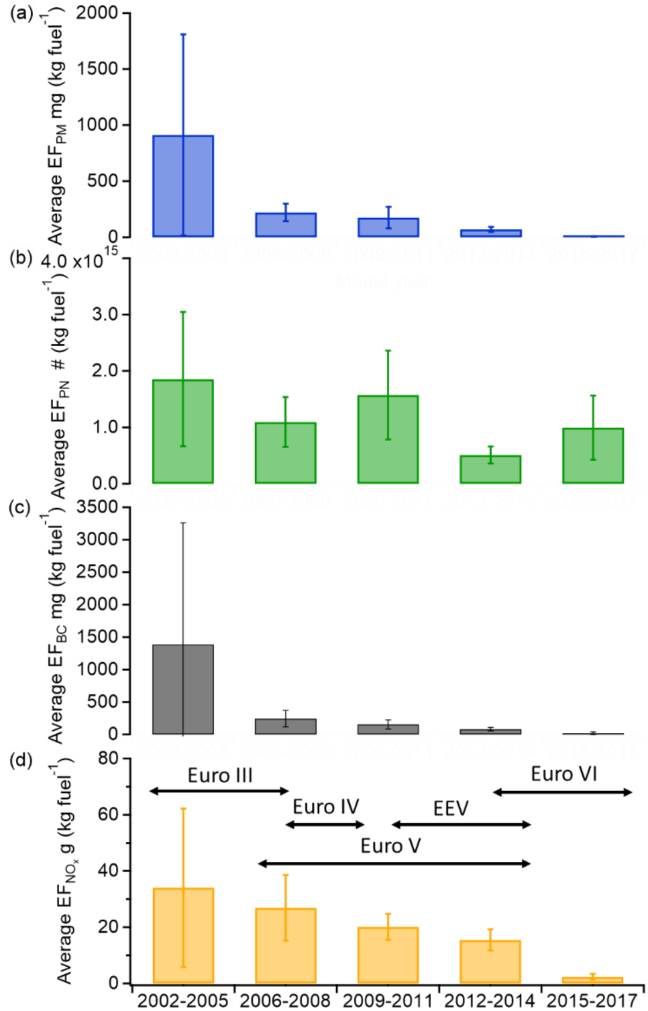

Figure 6. Changes of average EFs of (a) PM, (b) PN, (c) BC and (d) NO_x with respect to the registration year of HDTs. Error bars represent the statistical 95% confidence interval. Black arrows mark the years that the particular type of HDT examined in this study was first registered.

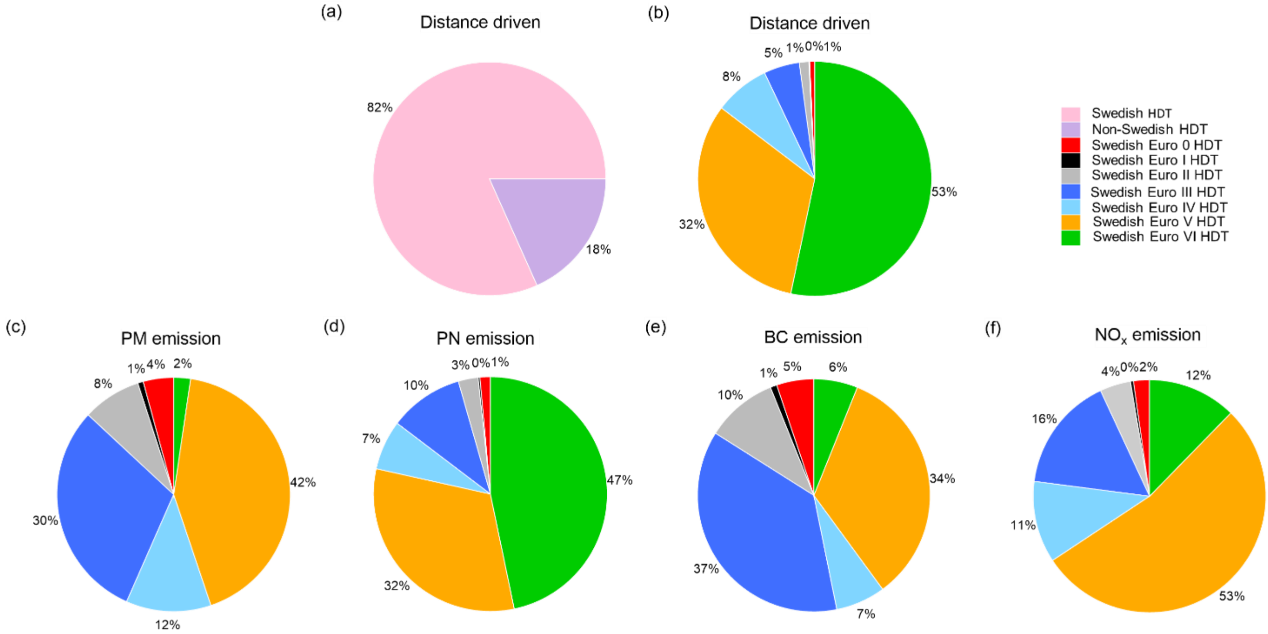

Figure 7. Relative contributions of kilometers driven by (a) Swedish and Non-Swedish HDTs and (b) Swedish Euro 0, Euro I, Euro II, Euro III, Euro IV, Euro V and Euro VI HDTs on Swedish roads during 2018. Approximation of contributions of pollutants emitted from Swedish HDTs in each Euro class to the total (c) PM, (d) PN, (e) BC and (f) NO_x emissions.